Tropospheric Ozone Over the North Pacific From Ozonesonde Observations

S. J. Oltmans[1], B. J. Johnson[1], J. M. Harris[1], A. M. Thompson[2], H. Y. Liu[3], C. Y. Chan[4], H. Vömel[1,5], T. Fujimoto[6], V. G. Brackett[7], W. L. Chang[8], J.-P. Chen[9], J. H. Kim[10], L. Y. Chan[5], H.-W. Chang[11]

[1]NOAA, Climate Monitoring and Diagnostics Laboratory, 325 Broadway, Boulder, CO 80305, samuel.j.oltmans@noaa.gov

[2]NASA Goddard Space Flight Center, Code 916, Greenbelt, MD 20771

[3]National Institute of Aerospace, Hampton, VA 23666

[4]Dept. of Civil and Structural Engineering, The Hong Kong Polytechnic University, Hung Hom, Hong Kong, China

[5]CIRES, University of Colorado and NOAA/CMDL, Boulder, CO 80309

[6]Japan Meteorological Agency, Tokyo, Japan

[7]SAIC, NASA/LaRC, Hampton, VA 23681

[8]Hong Kong Observatory, Hong Kong, China

[9]National Taiwan University, Taipei, Taiwan

[10]Pusan National University, Pusan, Korea

[11]Central Weather Bureau, Taipei, Taiwan

Submitted to the *Journal of Geophysical Research - Atmospheres*

TRACE-P Special Section

Revised October 2003

ABSTRACT: As part of the TRACE-P mission, ozonesondes were used to make ozone vertical profile measurements at nine locations in the North Pacific. At most of the sites there is a multi-year record of observations. From locations in the western Pacific (Hong Kong; Taipei; Jeju Island, Korea; and Naha, Kagoshima, Tsukuba, and Sapporo, Japan), a site in the central Pacific (Hilo, HI), and a site on the west coast of the U.S. (Trinidad Head, CA) both a seasonal and event specific picture of tropospheric ozone over the North Pacific emerges. Ozone profiles over the north Pacific generally show a prominent spring maximum throughout the troposphere. This maximum is tied to the location of the jet stream and its influence on stratosphere-troposphere exchange, and the increase in photochemical ozone production through the spring. Prominent layers of enhanced ozone in the middle and upper troposphere north of about 30N seem to be more closely tied to stratospheric intrusions while biomass burning leads to layers of enhanced ozone in the lower and upper troposphere at Hong Kong (22N) and Taipei (25N). The lower free tropospheric layers at Hong Kong are associated with burning in S.E. Asia but the upper layer may be associated with either equatorial N.H. burning in Africa or S. E. Asian biomass burning. In the boundary layer at Taipei very high mixing ratios of ozone were observed that result from pollution transport from China in the spring and local urban pollution during the summer. At the ozonesonde site near Tokyo (Tsukuba – 36N) very large enhancements of ozone are seen in the boundary layer in the summer that are characteristic of urban air pollution. At sites in the mid and eastern Pacific the signature of transport of polluted air from Asia is not readily identifiable from the ozonesonde profile. This is likely due to the more subtle signal and the fact that from the ozone profile and meteorological data by themselves it is difficult to identify such a signal.

During the TRACE-P intensive campaign period (February-April 2001), tropospheric ozone amounts were generally typical of those seen in the long-term records of the stations with multi-year soundings. The exception was the upper troposphere over Hong Kong and Taipei where ozone amounts were lower in 2001.

Introduction

Major population and industrial centers in Asia and North America surround the North Pacific basin. Continental Asia and western coastal North America are known to be major sources of emissions of compounds that are precursors to ozone formation. In addition the North Pacific is a dynamically active region with major storm tracks that often carry cyclonic disturbances from Asia toward North America [Fuelberg et al., 2003]. These disturbances are a significant mechanism for exchange from the stratosphere into the troposphere. In addition the large anticyclone located over the Pacific sends air from Asia toward North America. The transport patterns have a strong seasonal variation so that transport across the Pacific from Asia toward North America is strongest during the winter and spring months while transport from tropical and subtropical to more northerly latitudes is dominant during the summer.

The goals of this paper are to identify significant climatological features of the multiyear record of ozonesondes, provide a context for the TRACE-P aircraft campaign in February to April 2001, and present case studies of individual ozonesonde profiles. The case studies illustrate relevant processes that often produce the dramatic, layered vertical structure that is common in the individual profiles.

Measurements

Ozone is unique among the reactive atmospheric constituents in that it is relatively easily measured and there are regular measurements over longer periods of time. Vertical profiles of ozone were measured using ozonesondes at nine locations over the North Pacific during the Transport and Chemical Evolution over the Pacific (TRACE-P) period. Seven of these sites have multi-year records that have observations throughout

the course of the year. Seven of the nine sites were located in the western Pacific consistent with the major focus of TRACE-P [Jacob et al., 2003]. One site was located in Hawaii and another on the western coast of northern California. Information on the location and observation record of the ozonesonde sites is summarized in Table 1 and figure 1. Two other ozonesonde sites were operated in China during the TRACE-P period that are not reported on here, but are included in a paper by Chan et al. [2003b]. Ozone was measured using electrochemical sensors coupled with meteorological radiosondes flown on balloons. Most observations were done on a weekly schedule with some enhancements during the period of aircraft observations of TRACE-P. Extensive information on ozonesonde performance can be found in Harris et al. (1998). Under most circumstances the accuracy of ozonesonde measurements is 10% or better in the troposphere.

Approach

To identify possible transport pathways, backward air trajectories were calculated for several of the sites. These trajectories were used to study individual features seen in the ozone profile as well as provide information on average transport pathways. The method for calculating the trajectories, as well as a discussion of the limitations of trajectories for determining transport paths, appears in Harris and Kahl [1994]. An objective clustering technique [Moody, 1986] as implemented with NOAA/CMDL isentropic trajectories [Harris and Kahl, 1994] was employed to determine average transport pathways from ECMWF meteorological fields. Cluster analysis is a multivariate statistical method that separates trajectories into groups of clusters by maximizing the similarity of cluster members (both length and shape) while keeping the groups as

distinct as possible. The algorithm used (k-means clustering) does not result in the unique solution, but rather provides an objective approximation. As such the results are used as a tool to summarize trajectories not as immutable fact. The clustered trajectories are computed for a fixed arrival altitude at a site. With individual cases the NCEP-NCAR reanalysis [Kalnay et al., 1996] was used since data were available at greater height and time resolution (every six hours) for use in the three-hour trajectory calculation time step. Potential vorticity (PV), used to help identify the presence of stratospherically influenced air in the troposphere, was obtained from the NCEP reanalysis data which provides the PV information at 17 vertical intervals with a horizontal resolution of 2.5^0 of latitude and 2.5^0 of longitude. The reanalysis itself is T62 with 28 vertical levels. Climatological wind fields for the period 1991-2001 were generated from the Goddard Earth Observing System data assimilation system (GEOS DAS) at the NASA Data Assimilation Office [Schubert et al., 1993] as archived at the Harvard Atmospheric Chemistry Modeling Group (http://www-as.harvard.edu/chemistry/trop/geos/) [Bey et al., 2001].

Several key transport and chemical processes shape the ozone distribution at the ozone profiling sites, their influence varying with altitude and measurement location. Broad scale transport patterns and ozone precursor source regions are investigated, and the processes are illustrated with specific ozone profiles. In this study the mechanisms are suggestive rather than quantitative since detailed chemical and transport modeling is not included. Although a feature from a specific profile may be discussed in a section dealing with a particular mechanism, this does not imply it is the only process involved. The influences of biomass burning, meteorological transport, the stratosphere, background chemical ozone formation, and pollution, including outflow from the Asian continent and

urban pollution, are considered. Ozone behavior during Spring 2001 is also compared with longer-term characteristics of tropospheric ozone at several sites where a multiyear record is available.

Characteristics of North Pacific tropospheric ozone

Several recent publications have included a climatology of tropospheric ozone, based primarily on ozonesonde observations, from both a global [Logan, 1999; Fortuin and Kelder, 1998] and North Pacific perspective [Liu et al., 2002; Chan et al., 1998]. Here the focus is on the North Pacific and results from several stations not included in earlier studies are presented. A prominent feature of the ozone distribution in the troposphere at all of the North Pacific sites is the seasonal variation (Figure 3). Although there is a tendency toward spring maxima and autumn minima, this variation shows a dependence on altitude and location. At many of the sites, and in most seasons, there is a vertical gradient in ozone with the largest amounts in the upper troposphere and the smallest amounts near the surface. There are some notable exceptions to this when the upper troposphere shows a relative minimum or the boundary layer shows an enhancement.

At the sites north of 30N (Kagoshima – 32N, Tsukuba – 36N, Trinidad Head - 41N, Sapporo – 43N) during winter (Dec-Jan-Feb), spring (Mar-Apr-May), and autumn (Sep-Oct-Nov) the mid troposphere (3 – 6 km) shows similar behavior among the sites (figure 3a, b, d). The amounts vary with season but show very little difference between the stations within a season. The least variability at each individual site is also in this altitude region. During the summer there is both a large difference between locations and

high variability within the profile (figure 3c). In the upper troposphere (>8 km) the variability between stations and seasons shows a strong relationship to the tropopause height. At Kagoshima (32N), the most southerly of this group of stations, the higher tropopause height results in smaller ozone amounts above ~10 km for most months, while Sapporo (43N) has the largest amounts. It appears that in the region from 6 – 10 km the eastern Pacific site at Trinidad Head, California (41N) has less ozone in all seasons than is seen over Japan. In the lower troposphere (<3 km) during the spring, and to an even greater degree in summer, there is a significant enhancement (figure 2) at Tsukuba (36N) compared to the other locations (figure 3c).

At the three ozonesonde sites located to the south of 30N (Hilo – 20N, Hong Kong – 22N, Naha – 26N) the winter and spring seasons show similar profile shapes with a few ppb difference in mixing ratio at most altitudes (figure 4). In the spring Hong Kong (22N) has more ozone in the 2 – 6 km region, likely reflecting the significant influence of southeast Asian biomass burning on the this layer at Hong Kong as will be discussed later. In summer and autumn Hilo (20N) has a distinctly different profile shape than the other two sites with much less ozone in the upper troposphere (> 8 km) and a relative maximum in the mid troposphere. Within each season several processes are usually reflected in the averaged behavior that constitutes the kind of picture seen in figure 2. There may also be a shift in the dominant process from one season to the next, such as the availability of an ozone precursor source region or the characteristic flow pattern to the site. Although particular influences are considered separately the combination of factors that produce the seasonal variation and levels of ozone at a site will also be discussed.

Processes affecting tropospheric ozone over the North Pacific

In this section several of the distinctive characteristics of the seasonal and altitude distribution of tropospheric ozone over the North Pacific are investigated in terms of possible source or loss regions for ozone and patterns of transport that might influence the ozone profile. Particular attention is paid to biomass burning, large-scale meteorological transport, stratosphere-troposphere exchange, and pollution produced ozone. Processes not directly identifiable from the ozone profile and meteorological data considered in this paper are handled in a more general discussion section. Such a process is the overall buildup of ozone in the spring associated with increasing photochemical ozone production [Davis et al., 2003].

Biomass burning

There is an enhancement in ozone seen during late March and April in the 2-9 km layer at Hong Kong (22N) (Figure 2). This feature appears to be distinct from the broader seasonal maximum in the upper and middle troposphere. Such a feature may be weakly present at Naha (26N) but it does not show a clear separation from the broader seasonal maximum (Figure 2). Peaks are seen in this altitude range in individual profiles at Taipei (23N) as well. During winter and early spring, agricultural and land clearing burning takes place over northern Indochina along with episodic flow to the east that has been shown to have a marked influence on ozone measured over Hong Kong [Liu et al., 1999; Chan et al., 2000; Chan et al., 2002]. Fire counts (http://shark1.esrin.esa.it.ionia/FIRE/AF/ATSR/) for March 2001 (Figure 5) are illustrative of the burning activity that takes place in Southeast Asia and sub-Saharan Africa in the N.H. spring.

The ozone peak centered at about 8 km at Hong Kong may also be influenced by transport from Africa that can carry enhanced ozone from biomass burning as indicated by the fire count data. In addition lightning may contribute to the enhancement seen near 8 km. The outgoing long-wave radiation (OLR) data (http://www.cdc.noaa.gov/HistData/) show that in northern equatorial Africa there is a persistent band of low OLR (Figure 6), which is indicative of enhanced convective activity. Such activity is capable of lofting ozone precursors as well as producing lightning NO_x that may contribute to ozone formation [Liu et al., 2002]. Investigation of multiple years of fire count and OLR data found that the patterns seen in 2001 in figures 5 and 6 are quite representative of what takes place each year during the early spring. The episodic character of the ozone peaks can be traced to the sporadic nature of transport from the biomass burning source regions. The lower altitude portion of the enhanced layer is associated with transport from Southeast Asia. The upper portion of this layer may have multiple sources. Transport from both the Southeast Asian and African sources will be investigated in several individual cases. The combination of significant ozone precursor sources and favorable transport are likely contributors to the climatological ozone enhancement seen during March and April at the subtropical eastern Pacific ozonesonde sites, notably Hong Kong and Taipei. Similar conclusions have been reached based on model simulations [Liu et al., 2002]. Several case studies of significant enhancements during the spring at Hong Kong and Taipei are considered in the following discussion

The profile of March 17, 2000 at Hong Kong in the layer at 3 km (Figure 7) shows an ozone enhancement with a peak amount of about 90 ppb. The air parcel

trajectory (Figure 8) crosses over Southeast Asia with a travel time of about two days to Hong Kong after remaining relatively stagnant during the previous several days. A profile on March 27, 2001 launched at 0515 GMT (Figure 7) over Hong Kong (22N) shows less ozone than for the March 17, 2000 event but a very distinctive peak near 3 km nonetheless. The trajectory (Figure 9) is similar to that seen in March 2000 in that it passes over Southeast Asia but in this case the trajectory path moves slowly over northwestern Myanmar and then moves rapidly over northern Vietnam while ascending to the 3 km altitude where the enhanced ozone peak is seen over Hong Kong. The fire count map for March 2001 (figure 5) shows that the most intensive burning in Southeast Asia during this month was in western Myanmar, which based on the trajectory calculation is the origin of the air parcel reaching Hong Kong. This pattern is typical [Liu et al, 1999, 2002] of the layer of high ozone amounts seen over Hong Kong that results from biomass burning over northern Southeast Asia.

Plumes of enhanced ozone are not confined to the lower free troposphere but may also appear at substantially higher altitudes as is seen at Hong Kong on March 16, 2001 (Figure 7). The trajectory (Figure 10) shows the air parcel traveling over northern Indochina, extending over India, and within ~5 days back to northern Africa. Significant lifting of the air parcel is also necessary to form a layer at this altitude if the source of the ozone and/or its precursors is within the boundary layer. The source of the enhanced ozone amounts in the layer at 9-10 km over Hong Kong is not clear from the trajectory alone. Examination of the outgoing long-wave radiation (OLR) information shows little evidence of convection over northern Southeast Asia in the 1-2 days prior to the observation of the enhanced ozone layer over Hong Kong. This suggests that in this case

the burning region in closest proximity to Hong Kong may not be the source of the higher altitude peak. Northern equatorial Africa is also a region of significant biomass burning during this time of year and can also have significant convection. An ozone profile was obtained at Taipei on March 16, 2001 as well (Figure 11). An enhanced ozone layer was also seen at 9 km in this profile and the trajectory (Figure 12) looks very similar to that at Hong Kong with very rapid transport from northern Africa.

For the 9-11 km layer at Hong Kong on March 27, 2001 the air parcel trajectory for 0600 GMT passes over Southeast Asia, India and the Arabian Peninsula within two days, reaching central Africa within three days (Figure 13). West-central equatorial Africa is both a region of burning (Figure 5) [Duncan et al., 2003] and of convection based on the low values of OLR (Figure 6). Tropospheric column ozone is also enhanced near the region of high fire counts and convection in Nigeria as seen in the Tropical Tropospheric Ozone (TTO) map (Figure 14) from the TOMS observations (http://www.atmos.umd.edu/~tropo/) [Thompson and Hudson, 1999]. Very high TTO is also seen near the horn of Africa, which is the region that trajectories show as a possible source of the enhanced layer on March 16, 2001at Hong Kong and Taipei. It appears from the fire counts and the TTO maps that this region can be a significant source region for ozone. On the other hand, there is little evidence of convection based on OLR over northern Southeast Asia or India in the 1-2 days prior to the air parcel reaching Hong Kong. Because it was not possible to match fires with convection along the trajectory path in a precise way the influence of African burning on the ozone profile over Hong Kong is suggestive but not conclusive. There is, however, a good deal of consistency in the airflow patterns and source regions that produce the enhanced ozone layers over

Hong Kong. The influence of biomass burning in Africa as well as lightning were found to contribute to enhanced ozone in the upper troposphere at Hong Kong by Liu et al. [2002]. A modeling study [Liu et al., 2003] that looks at CO transport for observations made as part of the DC-8 aircraft measurements in TRACE-P on March 26, 2001 to the east of Hong Kong suggests that an enhanced layer of upper tropospheric CO was a result of convection over Southeast Asia. The OLR for March 25 shows strong convection over southern Laos. This is consistent with the finding of Liu et al. [2002] that S.E. Asian burning is an important source of upper tropopheric ozone enhancements over Hong Kong. Ozone enhancements in the upper troposphere at Hong Kong likely result from more than one source. For example, transport may deliver air influenced by southeast Asian burning that ultimately arrives under vigorous westerly flow from equatorial African regions that also experience significant burning as evidenced by fire counts.

Large-scale meteorological transport

Strongly varying meteorology plays an important role in the seasonal behavior of ozone. A climatology of seasonal flow patterns over the North Pacific at three altitudes (850, 500, and 200 hPa) provides a context for describing several of the features seen in the seasonal ozone behavior (Figure 15). At Kagoshima (32N) there is a strong seasonal ozone maximum in May throughout the troposphere, but in June below 5 km there is a sharp transition to lower ozone values that are accompanied by a sharp rise in humidity (not shown) that results from the switch to airflow from a more southerly, clean oceanic sector (Figure 15a). The late spring and late summer seasons show the strongest contrast in ozone (Figure 16) and also a large difference in transport pattern (Figure 17). At 4 km

during May (Figure 17a) there is no trajectory cluster in which air parcels remain over the ocean for a significant fraction of their travel time while in August (Figure 17b) 55% remain over the ocean for the full 10 days of the computed trajectory. The average ozone mixing ratio in May is 40 ppbv higher than in August at 4 km and reflects the significant ozone sink in the low latitude, summer marine atmosphere [Oltmans et al., 2001]. The higher May amounts reflect the longer lifetime of ozone during a period of increasing photochemical production [Davis et al., 2003]. At other altitudes, trajectories that remain over the ocean for the full 10 days are seen at least 45% of the time (at 12 km) to a high of more than 75% (at 1 km) in August. In May, on the other hand, only in the boundary layer do trajectories remain over the ocean (20% of the time).

The transition from continental to maritime flow is even more prominent at Naha (26N). Appearance of southerly flow south of 30N in the western Pacific at all levels leads to low summer ozone amounts in the troposphere. At Naha (26N) the minimum in the upper troposphere is in the winter (Figure 2). This corresponds to strong flow in the upper troposphere from low latitudes over the subtropical sites in the western Pacific (Figure 15c – panel labeled DJF) where ozone amounts are low [Oltmans et al., 2001]. This feature is also seen at Hong Kong (22N) and Taipei (25N) [Chan et al., 1998; Liu et al., 2002].

Stratospheric influence

At the sites north of 30N in most seasons there is a gradient with altitude with higher ozone amounts closest to the tropopause (based on the standard thermal definition) and lower amounts near the surface. The notable exception is the low altitude maximum

below 2km at Tsukuba, and high altitude minima seen in the summer. The most prominent extension of high ozone from the upper troposphere deep into the lower troposphere is seen at Kagoshima (32N) in May. At altitudes above about 5 km there appears to be a slight lag in the appearance of the seasonal maximum as one goes northward from Kagoshima (32N) to Sapporo (43N) with the highest values appearing in May at Kagoshima, May-June at Tsukuba (36N), and June-July at Sapporo. This may reflect the northward movement (Figure 15c) of the subtropical upper tropospheric wind maximum (jet stream) [Ding, 1994] and the contribution from stratosphere-troposphere exchange [Holton et al., 1995]. Between 13-16 km from March through June the influence of the stratosphere appears to dominate with average amounts greater than 90 ppbv [Pierce et al., 2003]. Some of the features seen at the west coast U.S. location (Figure 3) at Trinidad Head, California (41N) resemble those seen on the opposite side of the Pacific at Sapporo (43N), but there are also some differences. At both locations the seasonal maximum in the mid-troposphere is broad. At both sites there are large ozone amounts in the upper troposphere, and large tropospheric amounts extend to highest altitudes during the summer as the tropopause height moves upward. In spring through summer there is about a 2 km thick layer just below the tropopause with ozone in excess of 125 ppbv.

The region over the North Pacific is an area of active exchange of air from the stratosphere into the troposphere primarily in the winter and spring (Sprenger and Wernli, 2003; James et al. 2003). Several cases where stratospheric air appears to have influenced individual profiles are considered here. At Jeju Island (34N), in the Yellow Sea off the southwest coast of Korea, the profile of March 1, 2001 (Figure 18) has prominent

maxima at 5.5 km and 9 km, and elevated ozone amounts from 4 km up to the tropopause. This enhancement is likely associated with stratosphere-troposphere exchange (STE) [Danielsen and Mohnen, 1977; Stohl, et al., 2003]. An indicator of tropospheric air that may be influenced by the stratosphere is elevated levels of potential vorticity (PV). Various values of PV (1 PV Unit = 10^{-6} m^2 s^{-1} K kg^{-1}) are used to demark the separation between the stratosphere and troposphere with 2 PVU a common value (Stohl et al., 2003). Here regions with PV of 1 PVU or greater are used to indicate tropospheric air that has been influenced by stratospheric air. Enhanced PV indicates the stratospheric origin of air over Jeju (34N) (Figure 19a). At 0600 GMT at a potential temperature (Θ) of 300 K (the potential temperature surface where the 5.5 km layer is seen at Jeju), a tongue of high PV (>1 PVU) stretches down over Korea. At Θ = 330 K (where the 9 km layer is seen) very high PV is seen well south of Korea and over Japan (Figure 19b). There is no sounding at Kagoshima at this time, but there is one at Tsukuba on March 2, 2001 with very high ozone (>300 pbbv) just above 7 km which is at Θ = 300 K. By March 2 the large ozone amounts are confined to altitudes above 10 km (the Θ = 330 K surface is in the stratosphere at ~ 11 km) at Jeju. The system responsible for the exchange event has moved rapidly eastward, but ozone amounts are still very high over Japan. This event has also been simulated by a Chemistry and Transport Model (CTM) [Wild et al., 2003] confirming the role of STE.

As noted earlier during the month of May Kagoshima has a very pronounced maximum in ozone through the entire troposphere in comparison with other months. Layers of enhanced ozone that exceed 100 ppbv often mark the profiles. Three profiles (Figure 20) were chosen that are representative of many of the May profiles over the 10-

year climatology used in this study. In all three cases the local tropopause (thermal) was at an altitude greater than 15 km, which is the usual case for May (see Figure 2). On May 20, 1999 there is an overall increase in ozone mixing ratio from ~40 ppbv at the surface to ~130 ppbv at 16 km. This "background" profile is similar to the long-term average for May (figure 16). Superimposed on the "background" profile are prominent peaks at approximately 3, 7, 10, and 12 km with maximum mixing ratios of 88, 133, 126, and 139 ppbv, respectively. At 3 km air has traveled rapidly from the north and descended significantly prior to reaching Kagoshima (Figure 21). Air parcel trajectories at 0000 and 0600 GMT show even more dramatic descent of 4 km in the two days prior to reaching the site. This corresponds with a strong surge of cool, dry air from Siberia. This layer has the marks of air that has recently descended from the stratosphere [Cooper et al., 1998]. The layer at 7 km also is very dry and has also descended (3 km) from aloft. On May 17, 2000 the ozone peak was at 7 km. The corresponding trajectory is very similar to the May 20, 1999 trajectory for a layer at the same altitude with descent of 3 km in the final two days before reaching Kagoshima (Figure 22). PV in the layer of high ozone mixing ratio is also enhanced (>1 PVU). On May 29, 2000 the air parcels in the layer at 4 km have also descended rapidly more than 5 km in the two days prior to reaching Kagoshima (32N). There are not elevated PV values in this layer at the time of the sounding. The air parcel travels from high latitudes (trajectory not shown) before arriving at Kagoshima. The complex path of the air parcel the three days prior to reaching the site makes it difficult to identify a source from the trajectory. The air parcel also descends over the Yellow Sea through a region of significant ozone precursor sources that may contribute to the ozone loading in this layer. In this case a mixture of sources may be responsible for

the elevated ozone amounts seen in this layer. In the layer from 6-10 km corresponding to low ozone amounts on May 29 the trajectories stay at latitudes south of Kagoshima passing over China, northern India and Africa, and the Atlantic. The trajectories or other meteorological data do not suggest a particular source of the lower ozone air other than the air parcels generally remaining at subtropical latitudes.

In the spring at Trinidad Head, California (41N) there is strong westerly flow in the upper troposphere (Figure 15c). Prominent peaks are seen in profiles such as the one for March 9, 2001 (Figure 23). These peaks are often associated with descending air parcels from the northwest (Figure 24). Potential vorticity (PV) in the 6-9 km layer (Figure 25) is enhanced over tropospheric values (>1 PVU). A low pressure system to the east of Japan and associated stratosphere-troposphere exchange on the flank of this low is the likely source of the ozone layer at 6-9 km seen at Trinidad Head.

At Hilo (20N) ozone profiles were obtained on both March 15 and 16, 2001 (Figure 26) showing a prominent ozone mixing ratio peak of 100 ppbv centered at 8 km on March 15, diminishing somewhat to ~85 ppbv on March 16. March 16 was the day that enhanced ozone amounts were seen at 9 km in the profile at Hong Kong (22N) and Taipei (25N) that may have resulted from biomass burning over Africa. The measurements at Hilo (~1830 GMT each day) bracket the time of the soundings at Hong Kong and Taipei (~0600 GMT on March 16). The trajectory for the air parcel reaching Hilo at 1800 GMT on March 15 and March 16 show the air parcel reaching the coast of China in about four days, well before the time of the soundings in Hong Kong and Taipei. A profile at 0245 GMT at Taipei on March 13 and another on the same day at Hong Kong at 0530 GMT each showed only a modest enhancement (mixing ratio of ~75 ppbv)

at about 9 km. Since the trajectory to Hilo went north of both Hong Kong and Taipei by ~5^{o} in latitude and 2-3 days earlier, the ozone peak at Hilo is likely not related to the same series of events leading to the ozone peaks seen at Hong Kong and Taipei. The PV map for March 15 shows a band of enhanced PV stretching from the coast of California westward to encompass Hawaii (Figure 27) near the altitude of the layer of high ozone observed in the soundings of March 15 and 16. This feature becomes a cutoff region of enhanced PV on March 16 over southern Hawaii. It appears that even at a relatively low-latitude site such as Hilo (20N), STE influenced the ozone distribution on this occasion.

Pollution events

Two types of pollution were tentatively identified in the ozone profiles based on the transport to the ozonesonde site. It was noted that at Tsukuba (36N) the average profile during the summer shows relatively high ozone amounts in the boundary layer (Figures 2 and 3). This summertime enhancement suggests that the large, nearby Tokyo population center that should be a large emitter of ozone precursors is a likely source of the elevated ozone amounts seen at Tsukuba [Logan, 1999]. During the summer at Taipei very high ozone amounts (>100 ppbv) are quite common in the lowest 2 km. The profile of August 7, 2000 (Figure 18) shows ozone in the boundary layer exceeding 160 ppb. Very weak circulation coming from off the ocean, relative humidity averaging more than 75% in the layer, and a surface temperature of 34C all suggest strong stagnation conditions that lead to photochemical ozone production associated with emissions in a large urban area. Although local pollution events are seen at Hong Kong (22N) during the summer none of the magnitude seen at Taipei (25N) was found in the ozonesonde record.

At Taipei (25N) on March 16, 2001 (Figure 18) the profile shows a boundary layer enhancement with a peak amount over 100 ppbv. In this case strong flow from the Asian continent (Figure 19) brings air to Taipei (25N). Prior to exiting the coast the air descends rapidly about 6 km in altitude. After the air parcel leaves the coast of the Asian continent it moves relatively slowly within the boundary layer to Taipei. In this case more than one source may be responsible for the elevated ozone amounts. A similar feature is not seen at Hong Kong (22N) for a profile obtained on the same day. Trajectories at the altitude of the maximum at Taipei are similar for both Hong Kong and Taipei. Both show air moving southward from China to the west of Korea over the Yellow Sea, a region noted for high levels of pollution. The trajectory passes through a slightly enhanced region of PV just north of the Yellow Sea as the air parcel begins its sharp descent. A CTM modeling study [Wild et al., 2003] shows that in addition to the significant pollution produced ozone, there is a stratospheric ozone signal associated with air descending on the backside of a cold front that passes over Taipei. Such outflow events are likely contributors to layers of enhanced ozone seen at the ozonesonde sites in the western Pacific and also illustrate the complex character of such layers when trying to attribute a mechanism or source for the enhancement.

Other mechanisms

Particular features in the ozone profile, whether the average profile or an individual case, in combination with available meteorological information may be suggestive of a possible mechanism for leading to the measured ozone feature. However, this approach is not suitable in many cases for arriving at causative mechanisms. An

important contributor to the spring ozone maximum in the troposphere is the increasing photochemical ozone production associated with increasing solar ultraviolet radiation [Davis et al., 2003; Wang et al., 1998]. Such a process is a much more dispersed influence that will not show up as a distinctive feature in an individual profile, but it is manifest in the overall seasonal pattern. At sites in the mid and eastern Pacific the signature of transport of polluted air from Asia is not readily identifiable from the ozonesonde profile. This is likely due to the more subtle signal and the fact that from the ozone profile and meteorological data by themselves, it is difficult to identify such a signal [Cooper et al., 2003]. Similarly the summertime draw-down reflects the greater influence of maritime air on these North Pacific sites as revealed in the dominant flow pattern (Figure 15) with a tendency to move air that is relatively depleted in ozone [Oltmans et al., 2001] into the region. The cutting off of potential continental sources suggests, that in the maritime environment under conditions with low levels of precursors, ozone loss will dominate over production.

The summer and autumn pattern in Hilo, Hawaii (20N) has many characteristics of a tropical location [Oltmans et al., 2001] with ozone through most of the troposphere relatively low (<40 ppbv) and values less than 10 ppbv in the marine boundary layer (Figure 4). However, in the spring ozone is enhanced to in excess of about 70 ppbv above 5 km. On average over the year and at all altitudes a large fraction of the trajectories spend 10 days over the Pacific Ocean prior to reaching Hawaii, ranging from more than 75% at 1 km to greater than 45% at 4 km. In the two months with the strongest contrast in ozone amount (Figure 29) at all altitudes (April and September) there are also differences in the transport pattern (Figures 30). In September at all altitudes at least 90% of the

trajectories remain over the ocean for 10 days. Below 4 km (Figure 30b) essentially all spend 10 days over the ocean. In April over-ocean trajectories are still prominent at low altitudes but, for example, at 4 km (Figure 30a) almost half reach the Asian continent, primarily China near 30N. The extent to which sources over the continent may influence the ozone concentration is difficult to determine [Harris et al., 1998, Chan et al., 2003a].

Representativeness of the TRACE-P aircraft campaign period

The two TRACE-P aircraft operated in the western Pacific from late February through early April 2001. In the first half of the period the planes operated out of Hong Kong (22N) and in the latter half from near Tokyo, Japan. Shown are the February-April 2001 averages compared with the longer-term 10-year record from one of the Japanese sites (Tsukuba – 36N) and the approximately 5-year record from Hong Kong (Figure 31). Of course the aircraft did not operate near any of these locations for the entire period so that the purpose here is to discern major differences between the tropospheric regime sampled in 2001 compared to the "average" behavior. At most of the sites the differences were very small and cannot be considered significant. The comparison shown for Tsukuba (36N) is representative of the small differences seen at most of the sites (Figure 31). Above 10 km at Kagoshima ozone amounts are several ppb lower than the 10-year average but this is a region of high variability both between individual profiles and from year-to-year. At Hong Kong (22N) there was a pronounced minimum at about 13 km in 2001 that is not seen in the longer-term average. This minimum was also present at Taipei during 2001 (not shown), although not as pronounced as at Hong Kong, indicating that this was not just a sampling artifact at a single site. Trajectories for the individual

profiles at the altitude of this upper tropospheric minimum show strong transport from the equatorial western Pacific for a number of the cases [Chan et al., 2003b]. The average seasonal flow patterns (not shown) for both the winter and spring of 2001 show enhanced flow in the upper troposphere from the tropics relative to the longer term averages depicted in figure 15c. The corresponding outgoing long-wave radiation (OLR) shows reduced OLR corresponding to significant convection over the region that the trajectories traverse in keeping with the more eastward displacement of the tropical convection during the weakening ENSO cold phase [Fuelberg et al., 2003]. It is likely that the air seen in the upper troposphere over Hong Kong and Taipei in many of the profiles in February – April 2001 has a low latitude source with air representative of the tropical upper troposphere [Oltmans et al., 2001]. The prevalence of such profiles in 2001 appears to be responsible for the minimum seen at 13 km in the average and reflects the lingering influence of the cold phase of ENSO [Liu et al., 2003; Fuelberg et al., 2003].

Between 9 – 10 km at Hong Kong there is an enhancement not seen in the longer-term average profile. This level was identified as one that may have resulted from biomass burning, perhaps over northern Africa. The year 2001 may thus be somewhat unusual in having this enhancement at this altitude. It is more common to see such features above about 10 km [Chan et al., 2000; Liu et al., 1999, 2002]. At mid and low tropospheric altitudes the average seasonal wind behavior in 2001 in the western Pacific appears typical of the 10-year average, which is reflected in the ozone behavior.

Conclusions

Ozone profiles over the north Pacific generally show a prominent spring maximum throughout the troposphere. This maximum is tied to the location of the jet stream and its influence on stratosphere-troposphere exchange, and the increase in photochemical ozone production through the spring. Prominent layers of enhanced ozone in the middle and upper troposphere north of about 30N seem to be more closely tied to stratospheric intrusions. Biomass burning, on the other hand, leads to layers of enhanced ozone in the lower and upper troposphere at Hong Kong (22N) and Taipei (25N). The lower free tropospheric layers at Hong Kong are associated with burning in S.E. Asia.The upper layer may be associated with either equatorial N.H. burning in Africa or S. E. Asian biomass burning. In the boundary layer at Taipei very high mixing ratios of ozone were observed that result from pollution transport from China in the spring and local urban pollution during the summer. At the ozonesonde site near Tokyo (Tsukuba – 36N) very large enhancements of ozone are seen in the boundary layer in the summer that are characteristic of urban air pollution. At sites in the mid and eastern Pacific the signature of transport of polluted air from Asia is not readily identifiable from the ozonesonde profile. This is likely due to the more subtle signal and the fact that from the ozone profile and meteorological data by themselves, it is difficult to identify such a signal. During the TRACE-P intensive campaign period (February-April 2001), tropospheric ozone amounts were rather typical of those seen in the long-term records of the stations with multi-year soundings; the exception was lower ozone amounts in the upper troposphere over Hong Kong and Taipei in 2001 when more transport from the tropics was observed, consistent with a weakening ENSO cold phase.

References:

Bey, I., D. J. Jacob, R. M. Yantosca, J. A. Logan, B. D. Field, A. M. Fiore, Q. Li, H. Y. Liu, L. J. Mickley, and M. G. Schultz, Global modeling of tropospheric chemistry with assimilated meteorology: Model description and evaluation, J. Geophys. Res., 106, 23,073-23,095, 2001.

Chan, L. Y., H. Y. Liu, K. S. Lam, T. Wang, S. J. Oltmans, and J. M. Harris, Analysis of the seasonal behavior of tropospheric ozone at Hong Kong, *Atmos. Environ., 32* , 159-168, 1998.

Chan, L. Y., C. Y. Chan, H. Y. Liu, S. Christopher, S. J. Oltmans, and J. M. Harris, A case study on the biomass burning in Southeast Asia and enhancement of tropospheric ozone over Hong Kong, *Geophys. Res. Lett., 27*, 1479-1482, 2000.

Chan, C. Y., L. Y. Chan, J. M. Harris, S. J. Oltmans, and D. R. Blake, Characteristics of biomass burning emission sources. transport and chemical speciation of enhanced springtime ozone profile of the troposphere over Hong Kong, *J. Geophys. Res.,108* (D1), 4015, doi10.1029/2001JD001555, 2003a.

Chan, C. Y., L. Y. Chan, W. L. Chang, Y. G. Zheng, H. Cui, X. D. Zheng, Y. Qin, and Y. S. Li, Characteristics of a tropospheric ozone profile and implications on the origin of ozone over subtropical China in the spring of 2001, *J. Geophys. Res., 108*(D20), 8800, doi:10.1029/2003JD003427, 2003b.

Cooper, O. R., J. L. Moody, J. C. Davenport, S. J. Oltmans, B. J. Johnson, X. Chen, P. B. Shepson, and J. T. Merrill, Influence of springtime weather systems on vertical ozone distributions over three North American sites, *J. Geophys. Res., 103*, 22,001-22,013, 1998.

Cooper, O. R., C. Forster, D. Parrish, M. Trainer, E. Dunlea, T. B. Ryerson, G. Hübler, F. Fehsenfeld, D. Nicks, J. Holloway, J. Nowak, C. Brock, J. de Gouw, C. Warneke, J. Roberts, F. Flocke, J. Moody, A case study of trans-Pacific warm conveyor belt transport: The influence of merging air streams on trace gas import to North America, *J. Geophys. Res., 108*(D22), doi:10.1029/2003JD000000, in press, 2003.

Danielsen, E. F. and V. A. Mohnen, Project Dustorm report: Ozone transport, in situ measurements and meteorological analyses of tropopause folding, *J. Geophys. Res., 82*, 5867-5877, 1977.

Davis, D. D. et al., Trends in western North-Pacific ozone photochemistry as defined by observations from NASA's PEM-West B (1994) and TRACE-P (2001) field studies, *J. Geophys. Res.,* accepted, 2003.

Ding, Y. H., *Monsoons over China*, Kluwer Acad. Norwell, Mass., 1994.

Duncan, B. N., R. V. Martin, A. C. Staudt, R. Yevich, and J. A. Logan, Interannual and seasonal variability of biomass burning emissions constrained by satellite observations, *J. Geophys. Res.,* 108(D2), 4100, doi:10.1029/2002JD002378, 2003.

Fortuin, J. P. and H. Kelder, An ozone climatology based on ozonesonde and satellite measurements, *J. Geophys. Res., 103*, 31,709-31,734, 1998.

Fuelberg, H. E., C. M. Kiley, J. R. Hannan, D. J. Westerberg, M. A. Avery, and R. E. Newell, Meteorological conditions and transport pathways during the Transport and Chemical Evolution over the Pacific (TRACE-P) experiment, *J. Geophys. Res., 108*(D20), 8782, do110.1029/2002JD003092, 2003.

Harris, J. M. and J. D. Kahl, Analysis of 10-day isentropic flow patterns for Barrow, Alaska: 1985-1992, *J. Geophys. Res., 99*, 25,845-25,855, 1994.

Harris, J. M., S. J. Oltmans, E. J. Dlugokencky, P. C. Novelli, B. J. Johnson and T. Mefford, An investigation into the source of the springtime tropospheric ozone maximum at Mauna Loa Observatory, *J. Geophys. Res., 25*, 1895-1898, 1998.

Harris, N., R. Hudson and C. Phillips, SPARC/GAW/IOC Assessment of Trends in Vertical Distribution of Ozone, *SPARC Report No. 1 and WMO Ozone Research and Monitoring Project Report No. 43*, Cedex, France, 1998.

Holton, J. R., P. H. Haynes, M. E. McIntyre, A. R. Douglas, R. B. Rood, and L. Pfister, Stratosphere – Troposphere Exchange, *Rev. Geophys., 33*, 403-439, 1995.

Hoell, J. M., D. D. Davis, S. C. Liu, R. E. Newell, H. Akimoto, R. J. McNeal, and R. J. Bendura, Pacific Exploratory Mission – West Phase B: February-March, 1994, *J. Geophys. Res., 102*, 28,223-28,240, 1997.

Jacob, D. J., J. H. Crawford, M. M. Kleb, V. S. Connors, R. J. Bendura, J. W. Raper, G. W. Sachse, J. C. Gille, L. Emmons, and J. C. Heald, The Transport and Chemical Evolution over the Pacific (TRACE-P) mission: Design, execution, and first results, *J. Geophys. Res., 108*(D20), 900, doi:10.1029/2002JD003276, 2003.

James, P., A. Stohl, C. Forster, S. Eckhardt, P. Seibert, and A. Frank, A 15-year climatology of stratosphere-troposphere exchange with a Lagrangian particle dispersion model 2. Mean climate and seasonal variability, *J. Geophy. Res. 108*(D12), 8522, doi:10.1029/2002JD002639, 2003.

Kalnay, E. et al., The NCEP-NCAR 40 year reanalysis project, *Bull. Am. Meteorol. Soc*., *77*, 437-471, 1996.

Liu, H, W. L. Chang, S. J. Oltmans, L. Y. Chan, J. M. Harris, On springtime high ozone events in the lower troposphere from Southeast Asian biomass burning, *Atmos. Environ., 33*, 2403-2410., 1999.

Liu, H., D. J. Jacob, L. Y. Chan, S. J. Oltmans, I. Bey, R. M. Yantosca, J. M. Harris, B. Y. Duncan, and R. V. Martin, Sources of tropospheric ozone along the Asian Pacific Rim: An analysis of ozonesonde observations, *J. Geophys. Res., 107*(D21), 4573, doi:10.1029/JD002005, 2002.

Liu, H., D. J. Jacob, I. Bey, R. M. Yantosca, B. N. Duncan, and G. W. Sachse, Transport pathways for Asian combustion outflow over the Pacific: Interannual and seasonal variations, *J. Geophys. Res., 108*(D20), 8786, doi:10.1029/2002JD003102, 2003.

Logan, J. A., An analysis of ozonesonde data for the troposphere: Recommendations for testing 3-D models and development of a gridded climatology for tropospheric ozone, *J. Geophys. Res., 104*, 16,115-16,149, 1999.

Moody, J., The influence of meteorology on precipitation chemistry at selected sites in the eastern United States, Ph.D. thesis, 176 pp., Univ. of Michigan, Ann Arbor, Michigan, 1986.

Newchurch, M. J., M. A. Ayoub, S. J. Oltmans, B. J. Johnson, F. J. Schmidlin, Vertical distribution of ozone at fours sites in the United States, *J. Geophys. Res. (in press)*, 2003.

Oltmans, S .J., et al., Ozone in the Pacific tropical troposphere from ozonesonde observations, *J. Geophys. Res., 106*, 32,503-32-525, 2001.

Pierce, R. B. et al., Regional Air Quality Modeling System (RAQMS) predictions of the tropospheric ozone budget over East Asia, *J. Geophys. Res., 108*(D21), 8825, doi:10.1029/2002JD003176, in press, 2003.

Schubert, S. D., R. B. Rood, and J. Pfaendtner, An assimilated data set for earth science applications, *Bull. Amer. Meteorol. Soc., 74*, 2331-2342, 1993.

Sprenger, M. and H. Wernli, A northern hemispheric climatology of cross-tropopause exchange for the ERA 15 time period (1979-1993), *J. Geophy. Res. 108*(D12), 8521, doi:10.1029/2002JD002636, 2003.

Stohl, A. et al., Stratosphere-troposphere exchange: A review, and what we have learned from STACCATO, *J. Geophy. Res. 108*(D12), 8516, doi:10.1029/2002JD002490, 2003.

Thompson, A. M. and R. D. Hudson, Tropical Troposphere Ozone (TTO) maps from Nimbus-7 and Earth Probe TOMS by the modified residual method: Evaluation with sondes, ENSO signals and trends from Atlantic regional time series, *Geophys. Res., 104*, 26,961-26,975, 1999.

Wang, Y., D. J. Jacob, and J. A. Logan, Global simulation of the tropospheric O_3-NO_X-hydocarbon chemistry, 3, Origin of tropospheric ozone and effects of non-methane hydrocarbons, *J. Geophys. Res., 103*, 10,757-10,768, 1998.

Wild, O., J. Sundet, M. J. Prather, I. Isaksen, H. Akimoto, E. V. Browell, and S. J. Oltmans, CTM ozone simulations for spring 2001 over the western Pacific: Comparisons with TRACE-P lidar, ozonesondes and TOMS columns, *J. Geophys. Res., 108*(D21), 8826, doi:10.1029/2002JD003283, in press, 2003.

Table 1: Locations and period of measurement for ozonesondes in the North Pacific.

Station	**Latitude**	**Longitude**	**Observations**	**No. of Obs.**
Hilo, Hawaii	19.4ºN	155.4ºW	1991-2001	452
Hong Kong, China	22.3ºN	114.3ºE	1993-2001	253
Taipei, Taiwan	25.0ºN	121.4ºE	2000-2001	62
Naha, Japan	26.2ºN	127.7ºE	1991-2001	408
Kagoshima, Japan	31.6ºN	130.6ºE	1991-2001	401
Jeju Island, Korea	33.5ºN	126.5ºE	2001	12
Tsukuba, Japan	36.1ºN	140.1ºE	1991-2001	594
Trinidad Head, Calif.	40.8ºN	124.2ºW	1997-2001	205
Sapporo, Japan	43.1ºN	141.3ºE	1991-2001	421

Figures:

Figure 1: Map locating the ozonesonde stations that were used in this study.

Figure 2: Average seasonal variation with altitude of the ozone mixing ratio at ozonesonde sites. Note the different altitude scale for Sapporo and Trinidad Head (0-15 km instead of 0-18 km). The solid dark line is the average tropopause height.

Figure 3: Average ozone vertical profiles by season at the four ozonesonde stations with longer-term records north of 30N. The symbol is the median value at 0.25 km altitude increments. For Kagoshima (x) the inner 50th percentile (25th to 75th percentile) of the data are plotted at each altitude as a horizontal line.

Figure 4: Average ozone vertical profiles by season at the three ozonesonde stations with longer-term records south of 30N. The symbol is the median value at 0.25 km altitude increments. For Naha (x) the inner 50th percentile (25th to 75th percentile) of the data are plotted at each altitude as a horizontal line.

Figure 5: Fire counts for March 2001 from the European Space Agency World Fire Atlas complied from observations made by the Along Track Scanning Radiometer (ATSR) on the ERS-2 satellite. The fire locations are the red dots.

Figure 6: Outgoing Longwave Radiation (OLR) data averaged for the 5-day period March 17-21, 2001 provided by the NOAA Climate Diagnostics Center. Low values of OLR are indicative of thick cloudiness associated with convective activity.

Figure 7: Profiles of ozone mixing ratio at Hong Kong on March 17, 2000, March 16, 2001, and March 27, 2001. The launch time of the ozonesonde for the three profiles was ~0530 GMT.

Figure 8: Isentropic 10-day back trajectory to Hong Kong on March 16, 2000 arriving at 3 km. The solid line is for the 0000 GMT trajectory and the dashed line for 0600 GMT.

Figure 9: Isentropic 10-day back trajectory to Hong Kong on March 27, 2001 arriving at 3 km at 0000 GMT.

Figure 10: Isentropic 10-day back trajectory to Hong Kong on March 16, 2001 at 0060 GMT arriving at 9 km.

Figure 11: Profiles of ozone mixing ratio at Taipei on August 7, 2000 at 0400 GMT and March 16, 2001 at 0700 GMT. The peak at 1 km on August 7 reached 162 ppbv.

Figure 12: Isentropic 10-day back trajectory to Taipei on March 16, 2001 arriving at 9 km. The solid line is for the 0000 GMT trajectory and the dashed line for 0600 GMT.

Figure 13: Isentropic 10-day back trajectory to Hong Kong on March 27, 2001 at 0060 GMT arriving at 10 km.

Figure 14: Tropical Troposheric Ozone (TTO) derived from the Earth Probe TOMS instrument.

Figure 15: Mean wind fields by season derived from the GEOS-DAS data for the period 1991 – 2001 for a) 850 hPa, b) 500 hPa, and c) 200 hPa.

Figure 16: Median monthly tropospheric ozone mixing ratio for May (open triangle) and August (solid diamond) for Kagoshima, Japan. The solid and dotted horizontal lines are the inner 50^{th} percentile of the mixing ratio at each 0.25 km altitude.

Figure 17: Average air parcel trajectories at 4 km altitude at Kagoshima for a) May and b) August based on data for 1991 – 2001 determined by clustering twice-daily trajectories. The percentage of the trajectories in each cluster is shown with the corresponding color symbol.

Figure 18: Profiles of ozone mixing ratio at Jeju Island on March 1, 2001 at 0415 GMT and March 2, 2001 at 0615 GMT. The median profile for the eight soundings obtained during March and April 2001 is also shown. The inner 50^{th} percentile (25^{th} to 75^{th} percentile) of the data is plotted at each altitude as a horizontal line.

Figure 19: Potential vorticity units on March 1, 2001 at 0600 GMT on the a) 300 K and b) 330 K potential temperature surfaces.

Figure 20: Profiles of ozone mixing ratio at Kagoshima on May 20, 1999, May 17, 2000, and May 29, 2000. The launch time of the ozonesonde for the three profiles was 1430 GMT.

Figure 21: Isentropic 10-day back trajectory to Kagoshima on May 20, 1999 arriving at 3.3 km. The solid line is for the 1200 GMT trajectory and the dashed line for 1800 GMT.

Figure 22: Isentropic 10-day back trajectory to Kagoshima on May 17, 2000 arriving at 7.3 km at 1800 GMT.

Figure 23: Profile of ozone mixing ratio at Trinidad Head on March 9, 2001 at 1800 GMT. The multiyear median profile for March is also shown. The inner 50^{th} percentile (25^{th} to 75^{th} percentile) of the data is plotted at each altitude as a horizontal line.

Figure 24: Isentropic 10-day back trajectory to Trinidad Head on March 9, 2001 at 1800 GMT arriving at 6 km.

Figure 25: Potential vorticity units on March 9, 2001 at 1800 GMT on the 315 K potential temperature surface.

Figure 26: Profiles of ozone mixing ratio at Hilo March 15 and 16, 2001. The launch time of the ozonesonde for the two profiles was 1830 GMT.

Figure 27: Potential vorticity units on March 15, 2001 at 1800 GMT on the 330 K potential temperature surface.

Figure 28: Isentropic 10-day back trajectory to Taipei on March 16, 2001 at 0060 GMT at 1 km.

Figure 29: Median monthly tropospheric ozone mixing ratio for April (open triangle) and September (solid diamond) for Hilo, Hawaii. The solid and dotted horizontal lines are the inner 50^{th} percentile of the mixing ratio at each 0.25 km altitude.

Figure 30: Average air parcel trajectories at 4 km altitude at Hilo for a) April and b) September based on data for 1991 – 2001 determined by clustering twice-daily trajectories. The percentage of the trajectories in each cluster is shown with the corresponding color symbol

Figure 31: Comparison of the February-March-April 2001 median ozone mixing ratio profiles with the long-term average for Hong Kong and Kagoshima. The inner 50^{th} percentile (25^{th} to 75^{th} percentile) of the data is plotted at each altitude as a horizontal line.

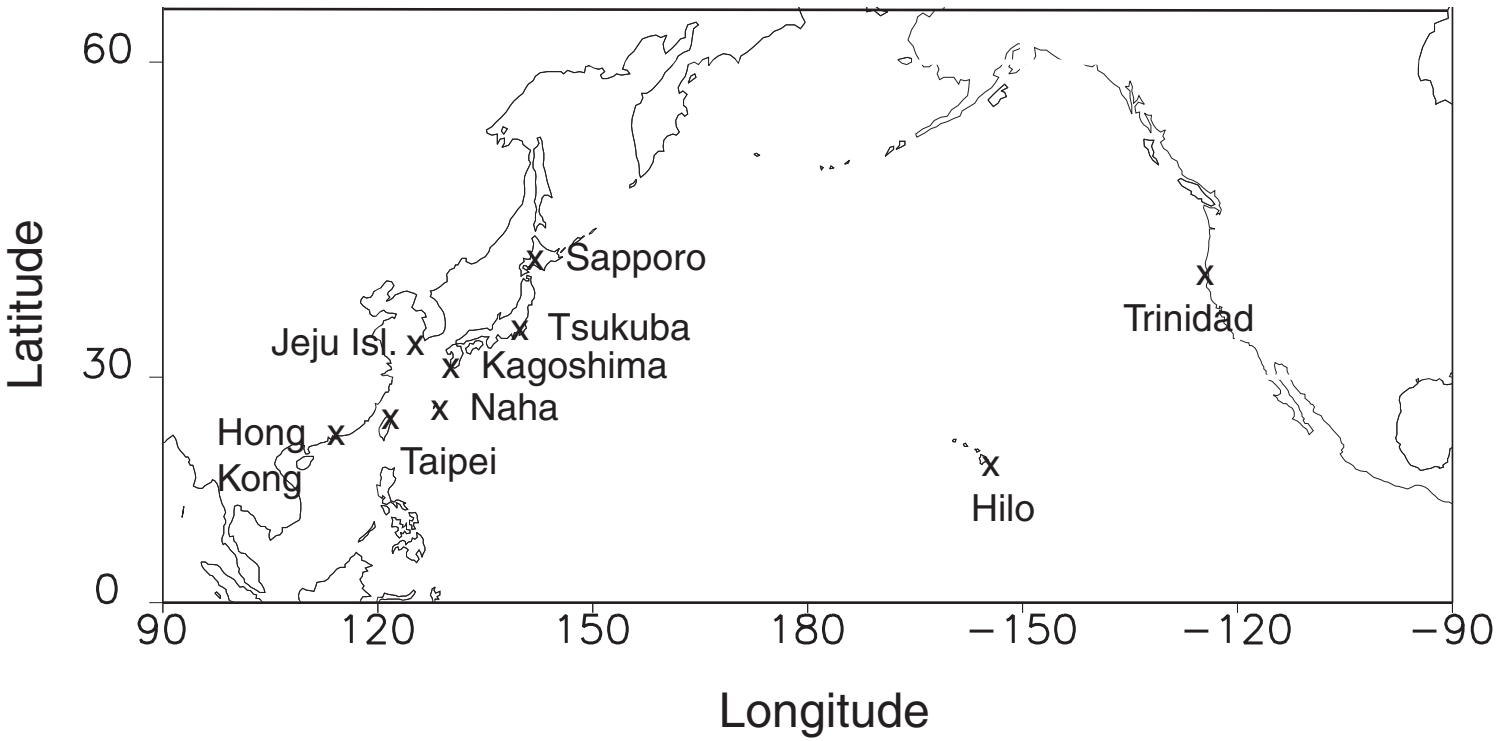

Figure 1: Map locating the ozonesonde stations that were used in this study.

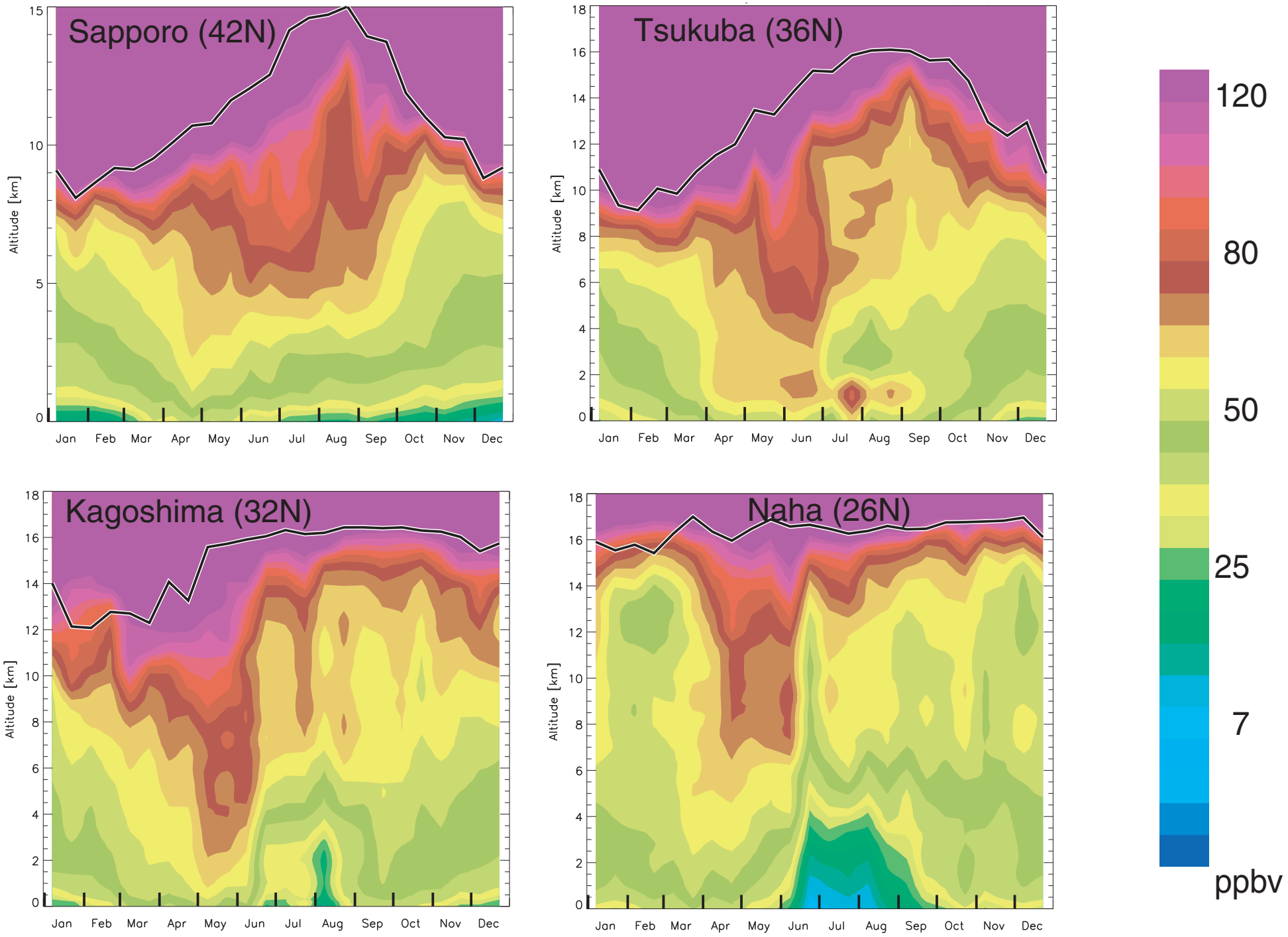

Figure 2: Average seasonal variation with altitude of the ozone mixing ratio at ozonesonde sites.

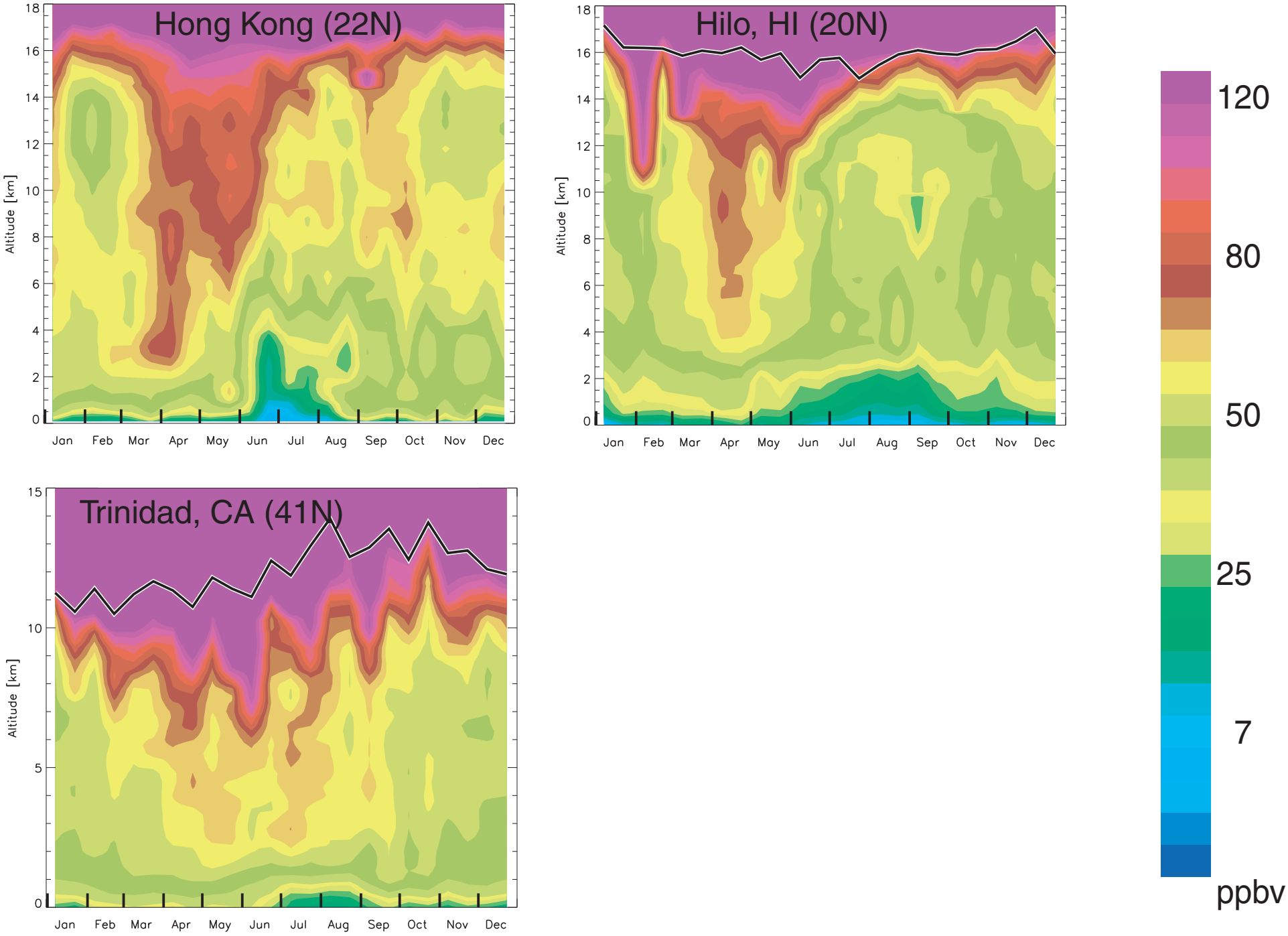

Figure 2 (continued)

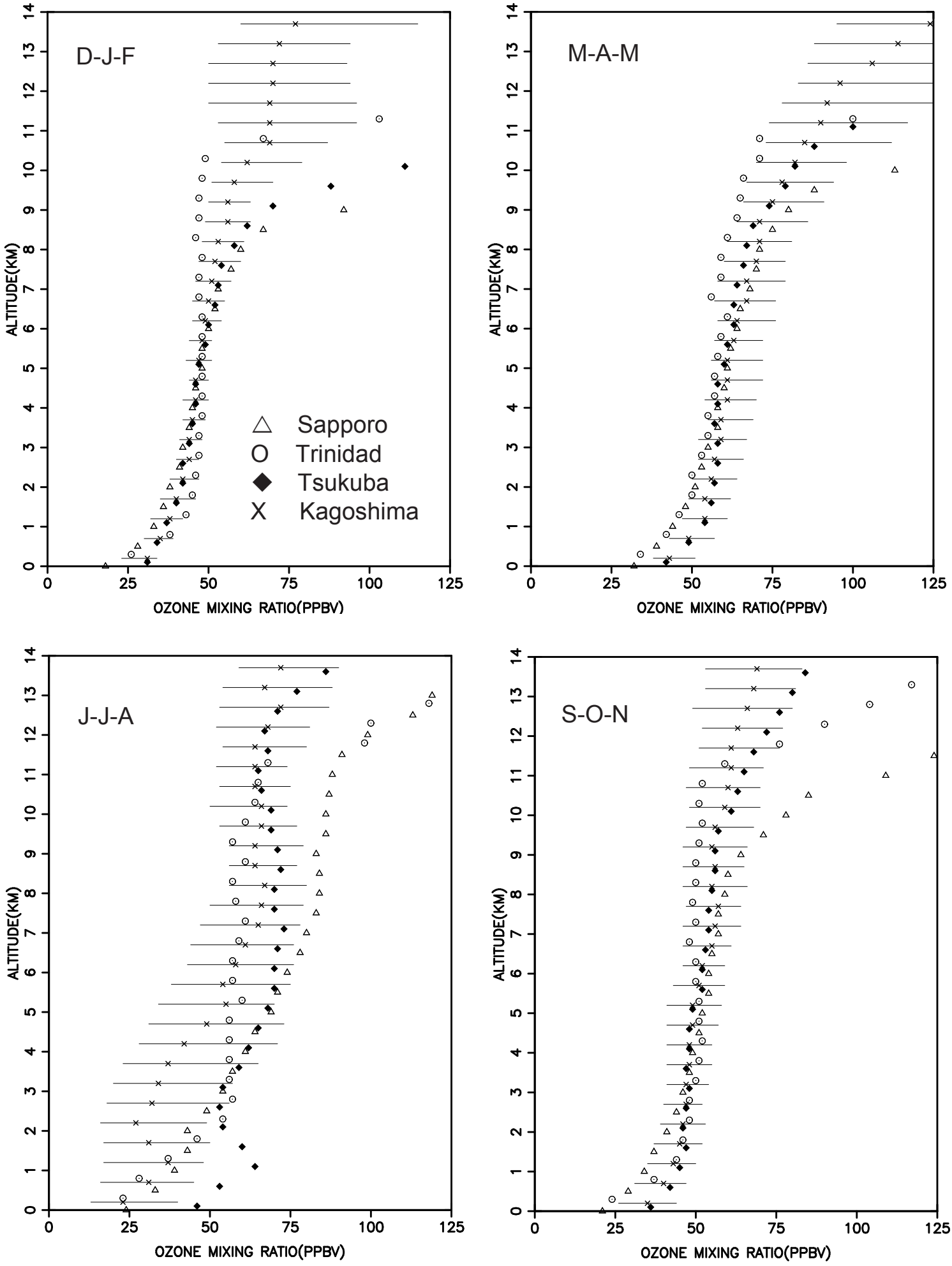

Figure 3: Average ozone vertical profiles by season at stations north of 30N.

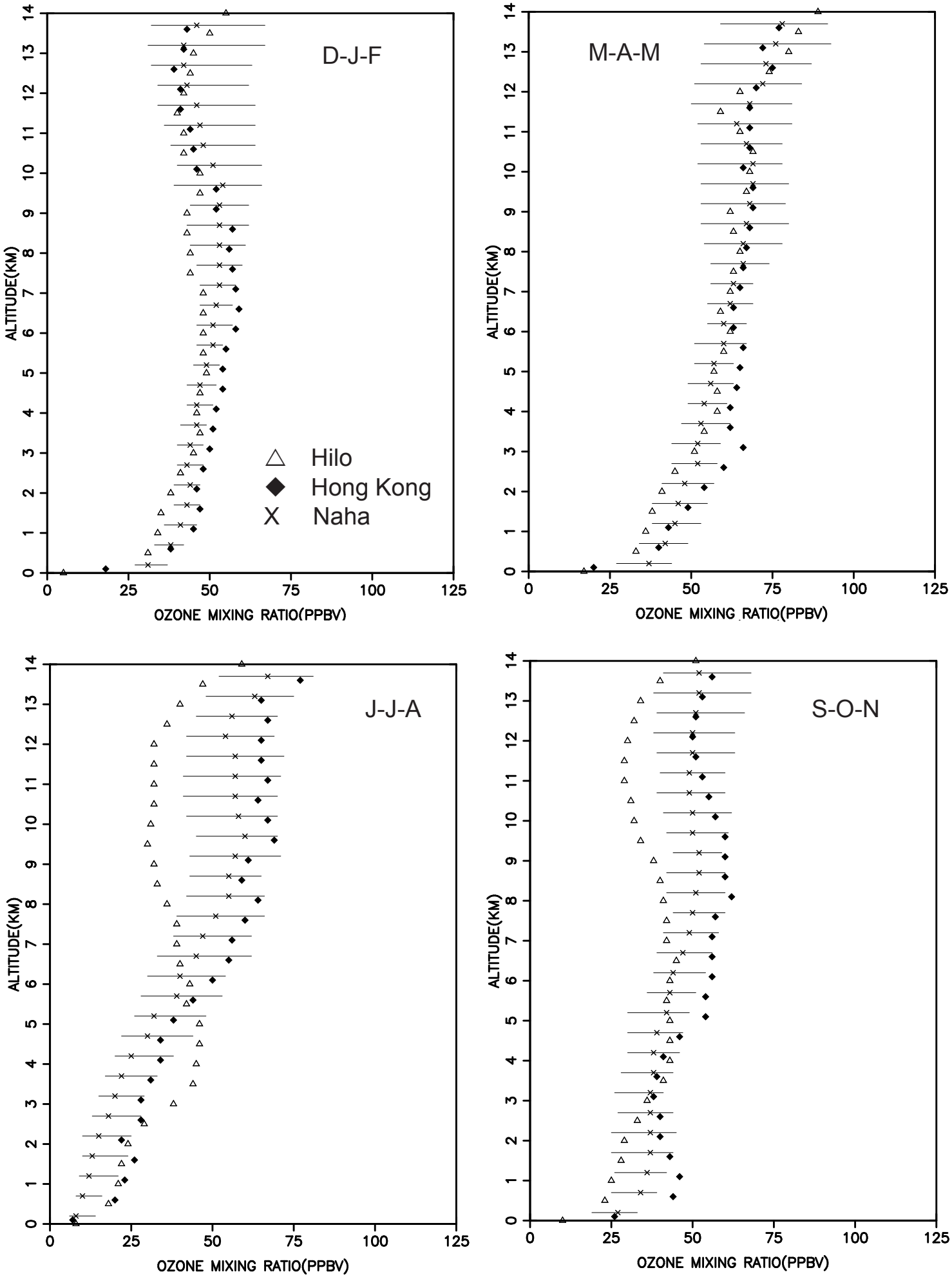

Figure 4: Average ozone vertical profiles by season at stations south of 30N.

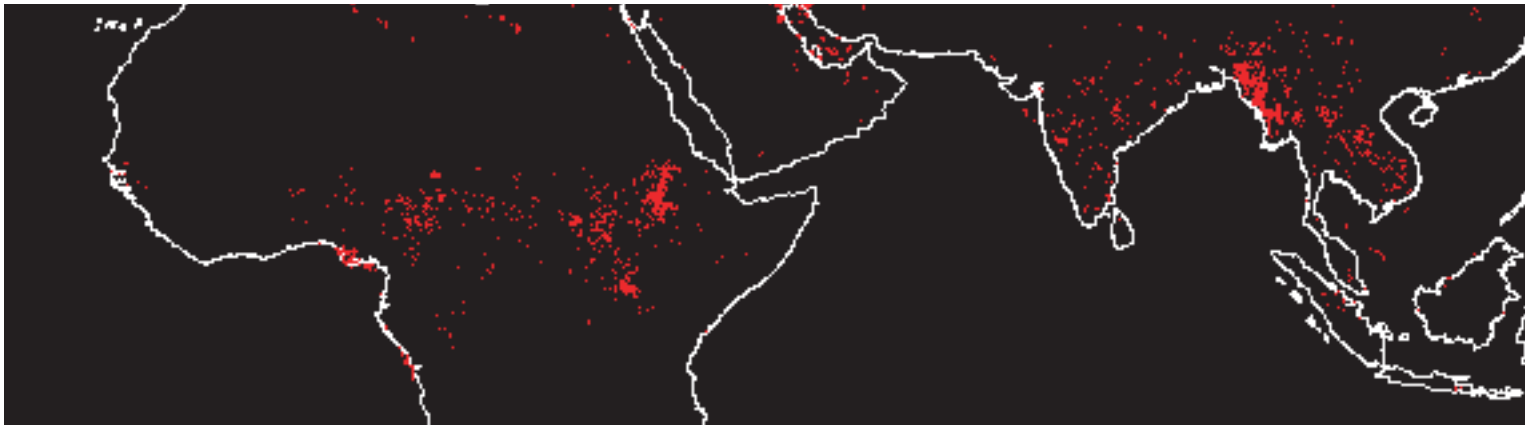

Figure 5: Fire counts for March 2001 from the European Space Agency World Fire Atlas complied from observations made by the Along Track Scanning Radiometer (ATSR) on the ERS-2 satellite. The fire locations are the red dots.

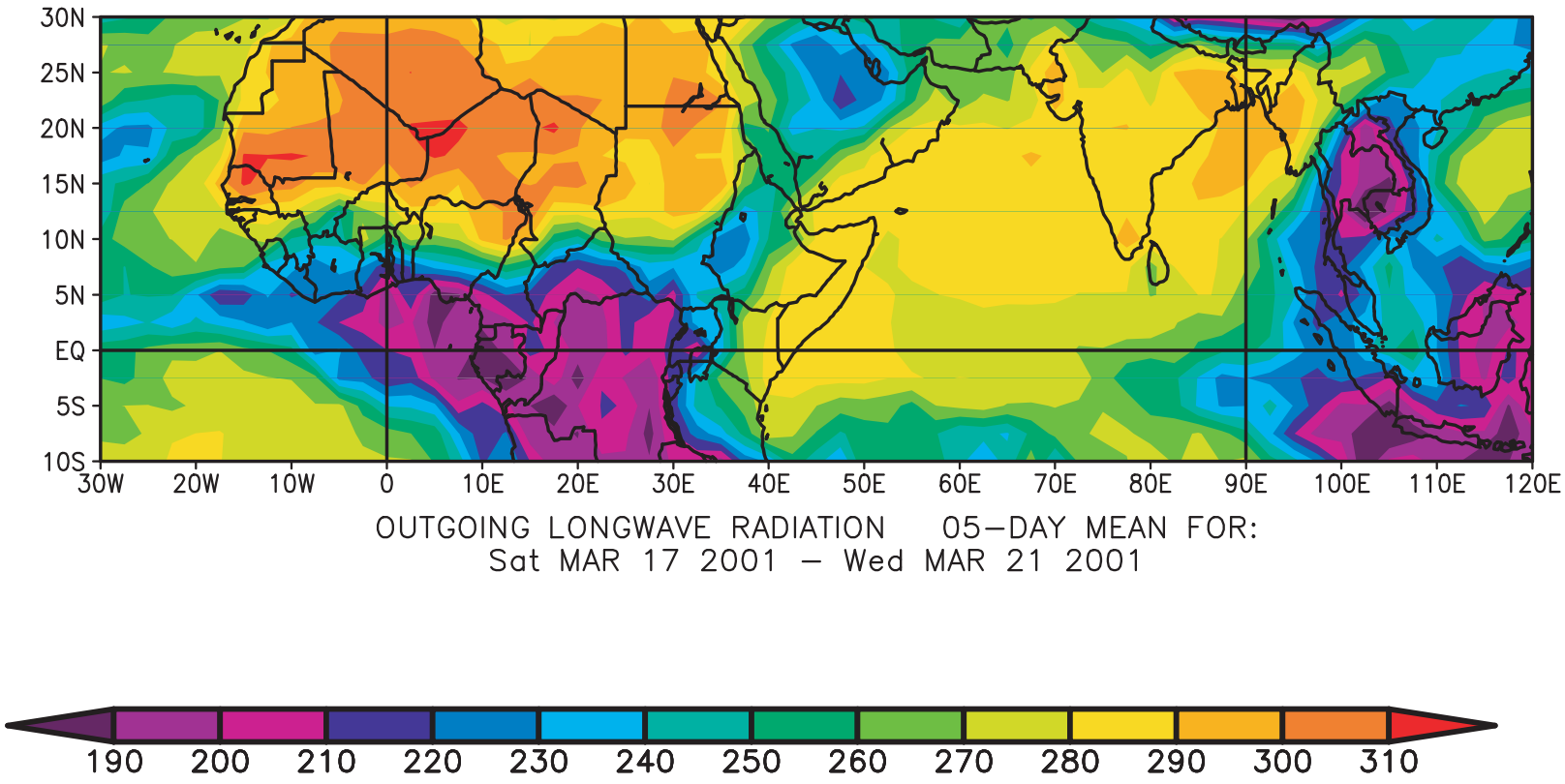

Figure 6: Outgoing Longwave Radiation (OLR) data averaged for the 5-day period March 17-21, 2001provided by the NOAA Climate Diagnostics Center. Low values of OLR are indicative of thick cloudiness associated with convective activity.

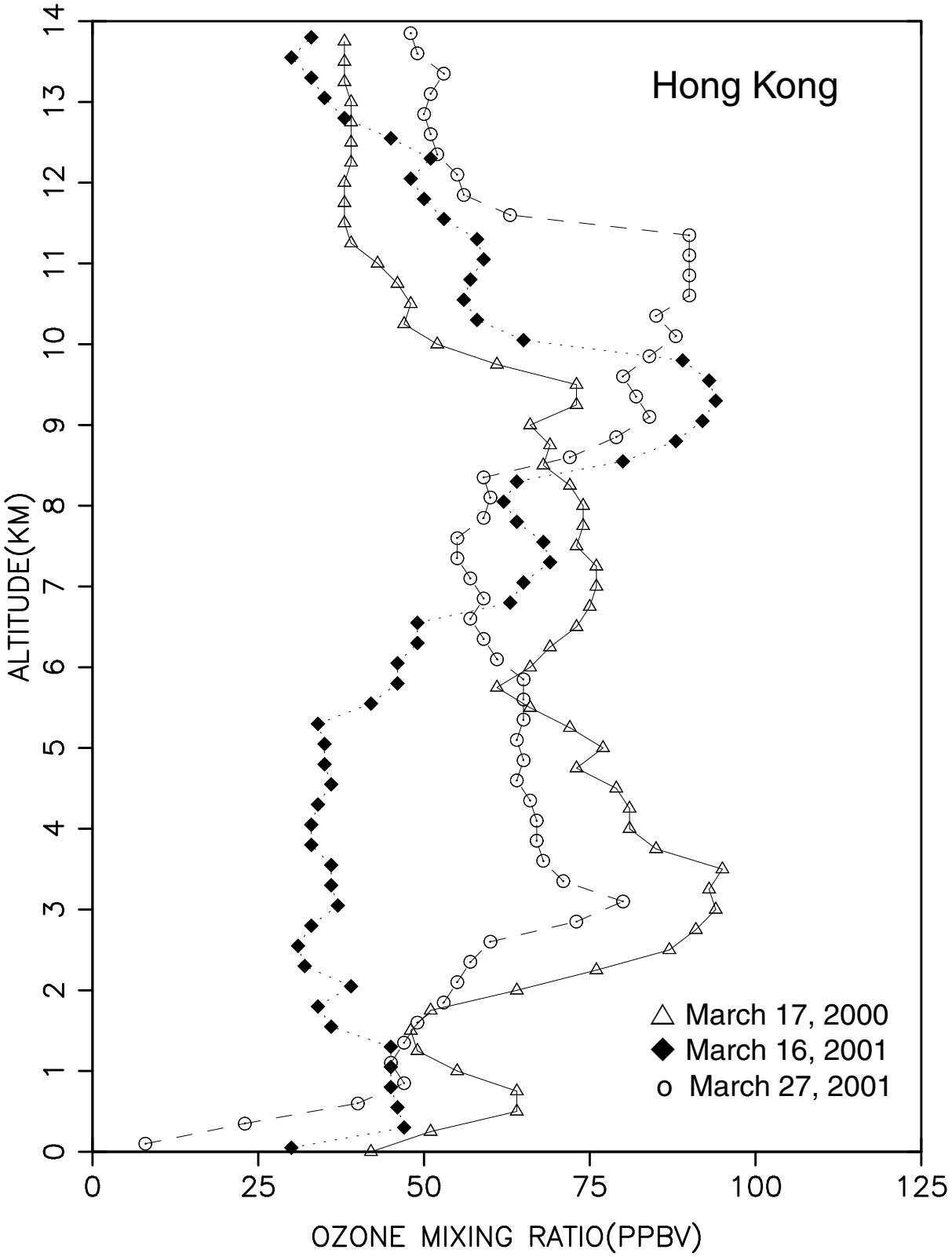

Figure 7: Profiles of ozone mixing ratio at Hong Kong on March 17, 2000, March 16, 2001, and March 27, 2001. The launch time of the ozonesonde for the three profiles was ~0530 GMT.

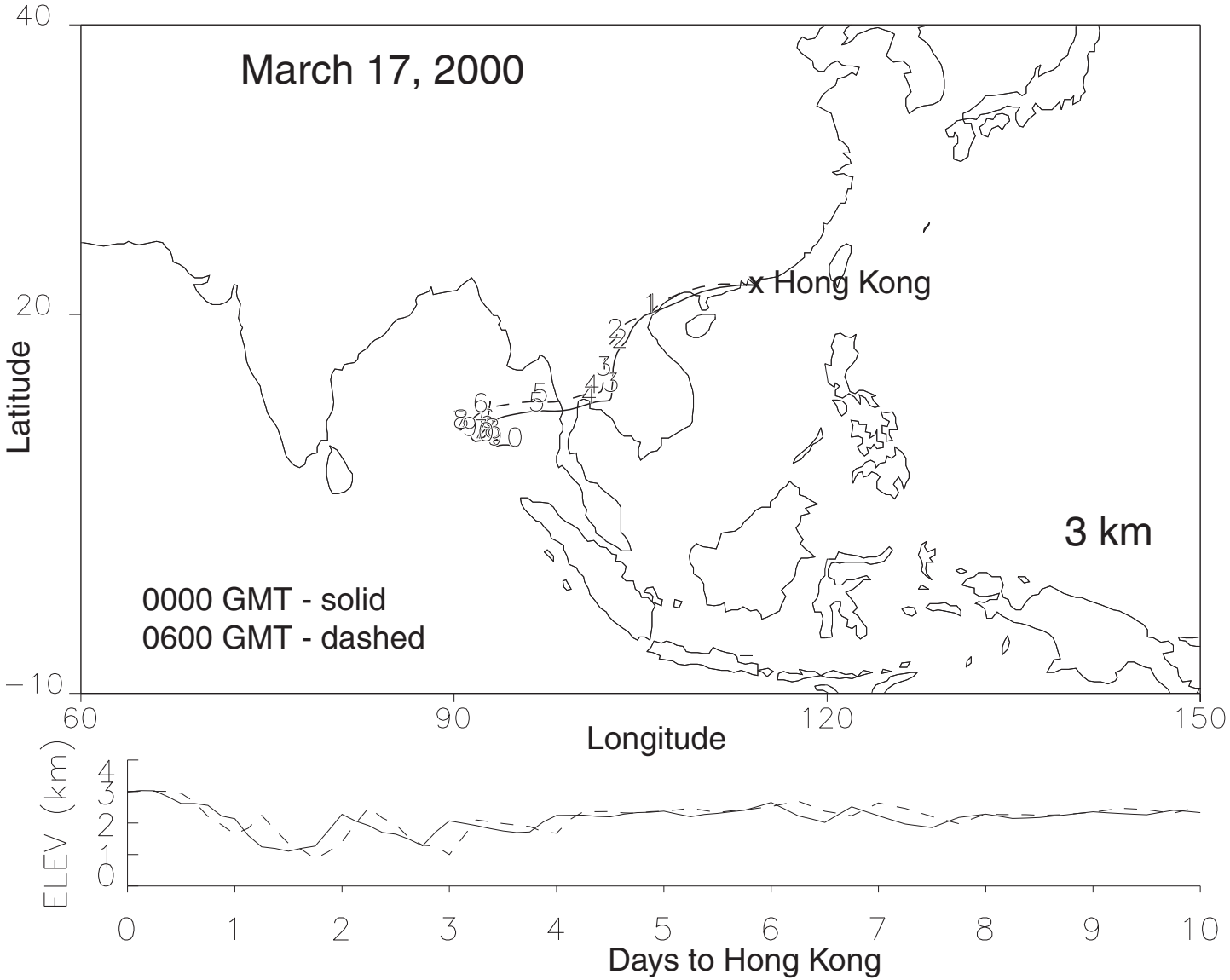

Figure 8: Isentropic 10-day back trajectory to Hong Kong on March 16, 2000 arriving at 3 km. The solid line is for the 0000 GMT trajectory and the dashed line for 0600 GMT.

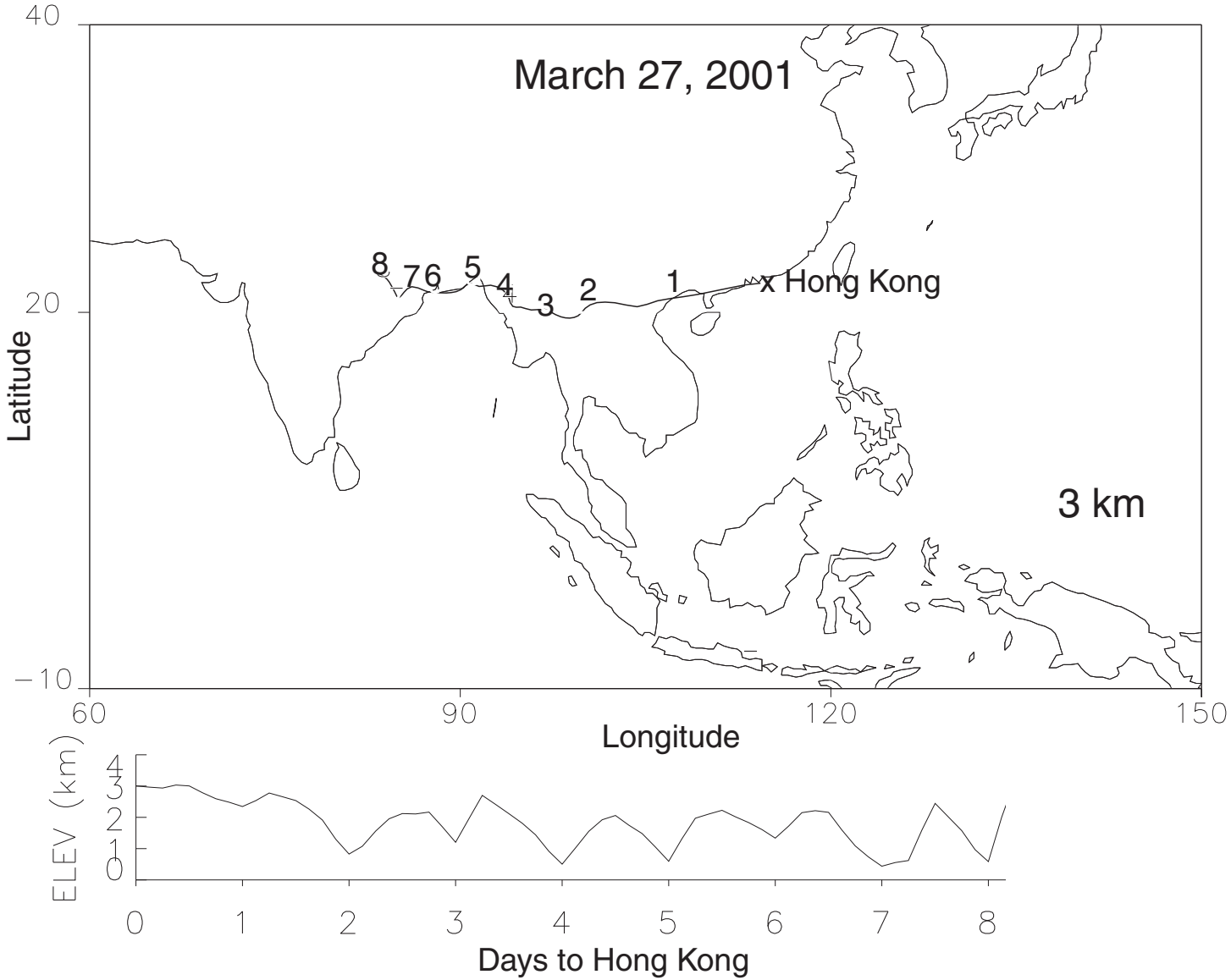

Figure 9: Isentropic 10-day back trajectory to Hong Kong on March 27, 2001 arriving at 3 km at 0000 GMT.

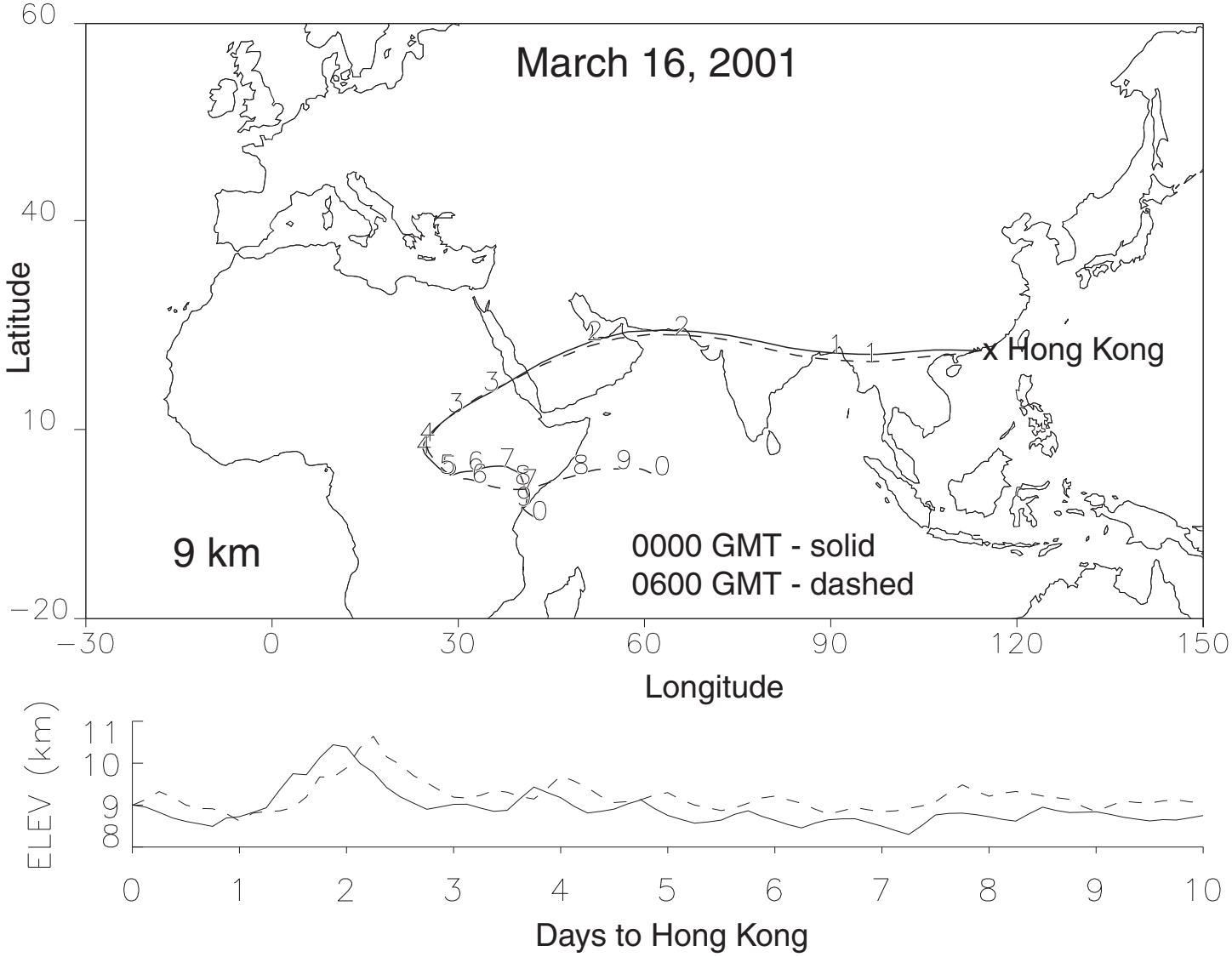

Figure 10: Isentropic 10-day back trajectory to Hong Kong on March 16, 2001 at 0060 GMT arriving at 9 km.

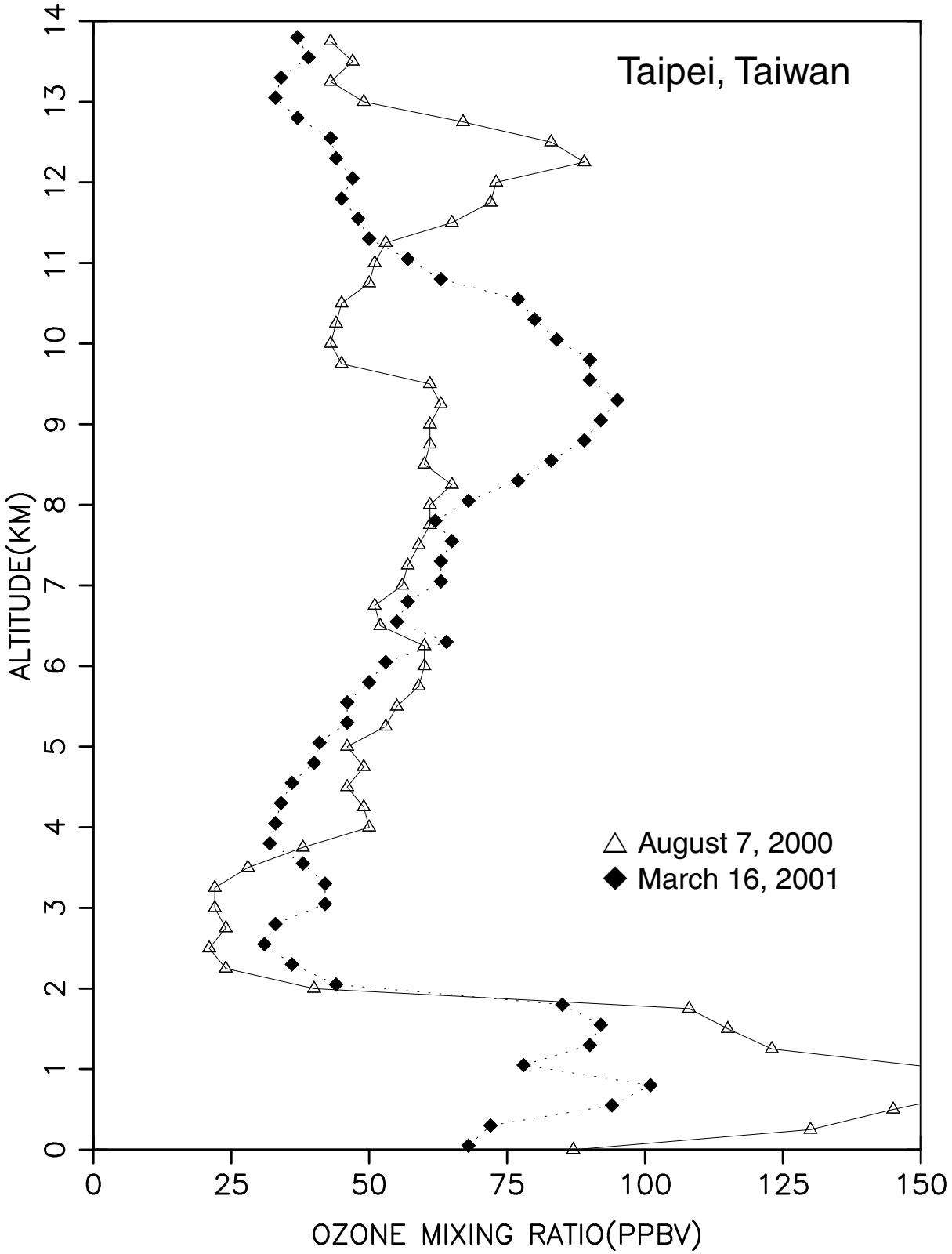

Figure 11: Profiles of ozone mixing ratio at Taipei on August 7, 2000 at 0400 GMT and March 16, 2001 at 0700 GMT. The peak at 1 km on August 7 reached 162 ppbv.

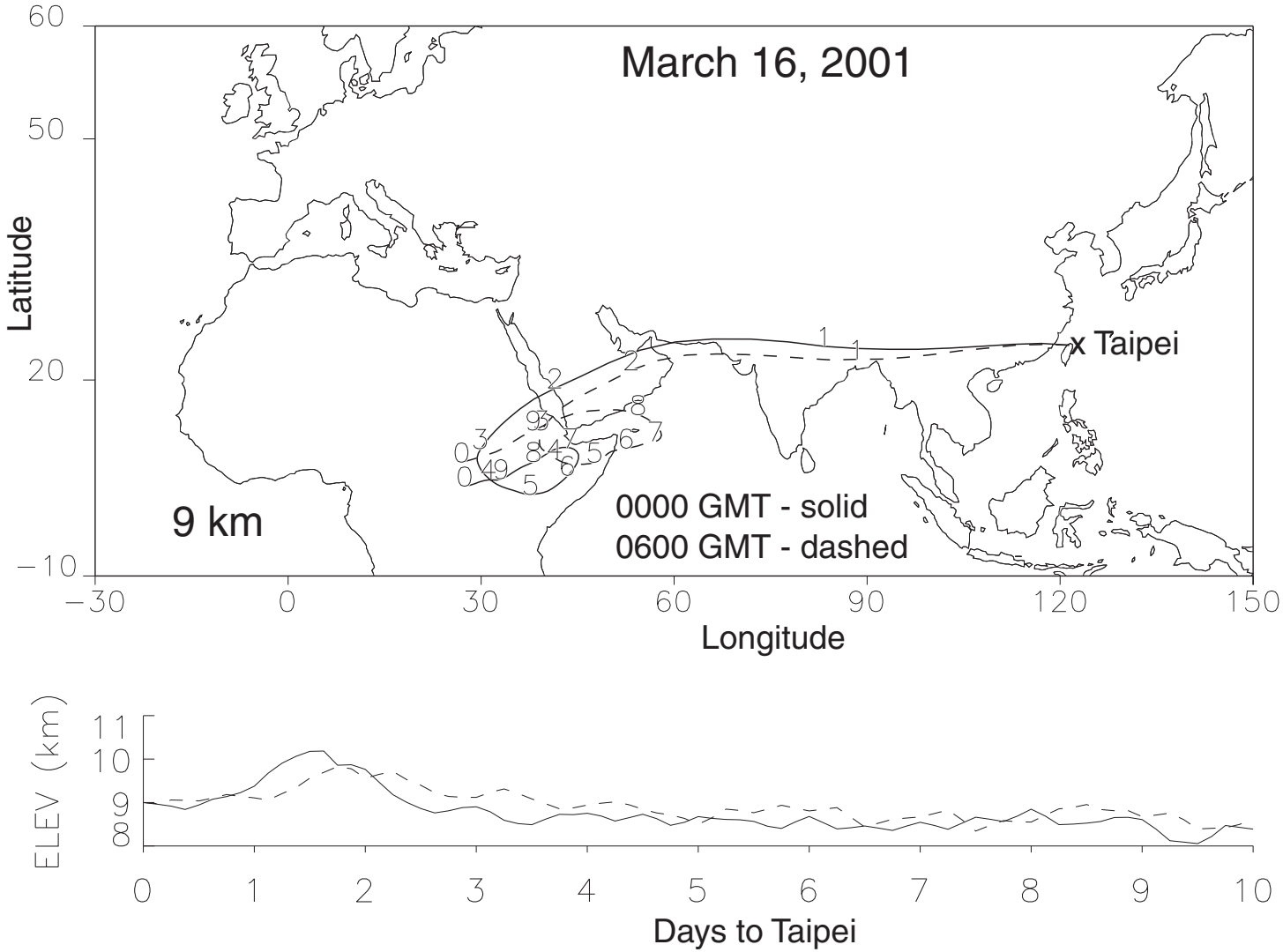

Figure 12: Isentropic 10-day back trajectory to Taipei on March 16, 2001 arriving at 9 km. The solid line is for the 0000 GMT trajectory and the dashed line for 0600 GMT.

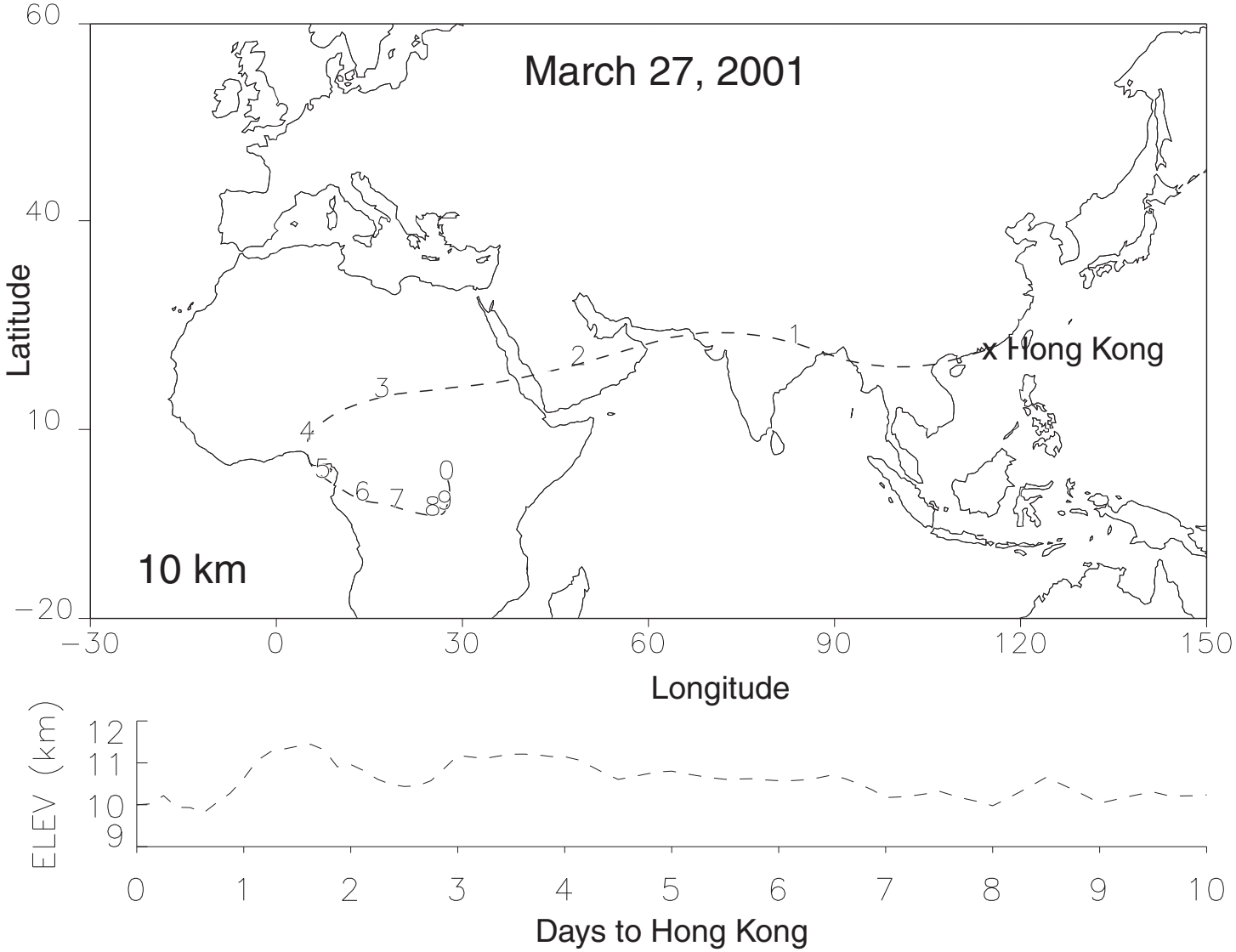

Figure 13: Isentropic 10-day back trajectory to Hong Kong on March 27, 2001 at 0060 GMT arriving at 10 km.

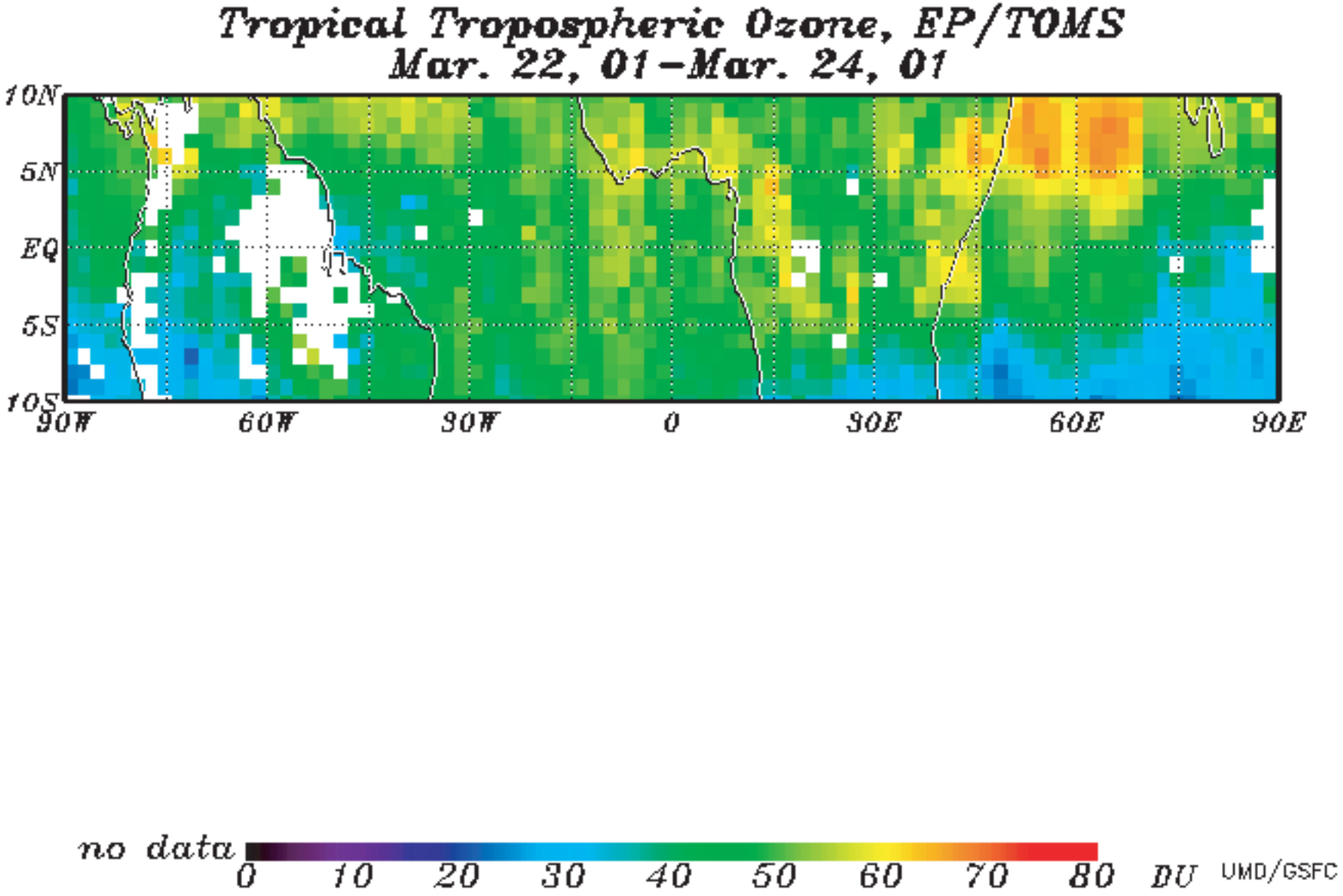

Figure 14: Tropical Troposheric Ozone (TTO) derived from the Earth Probe TOMS instrument.

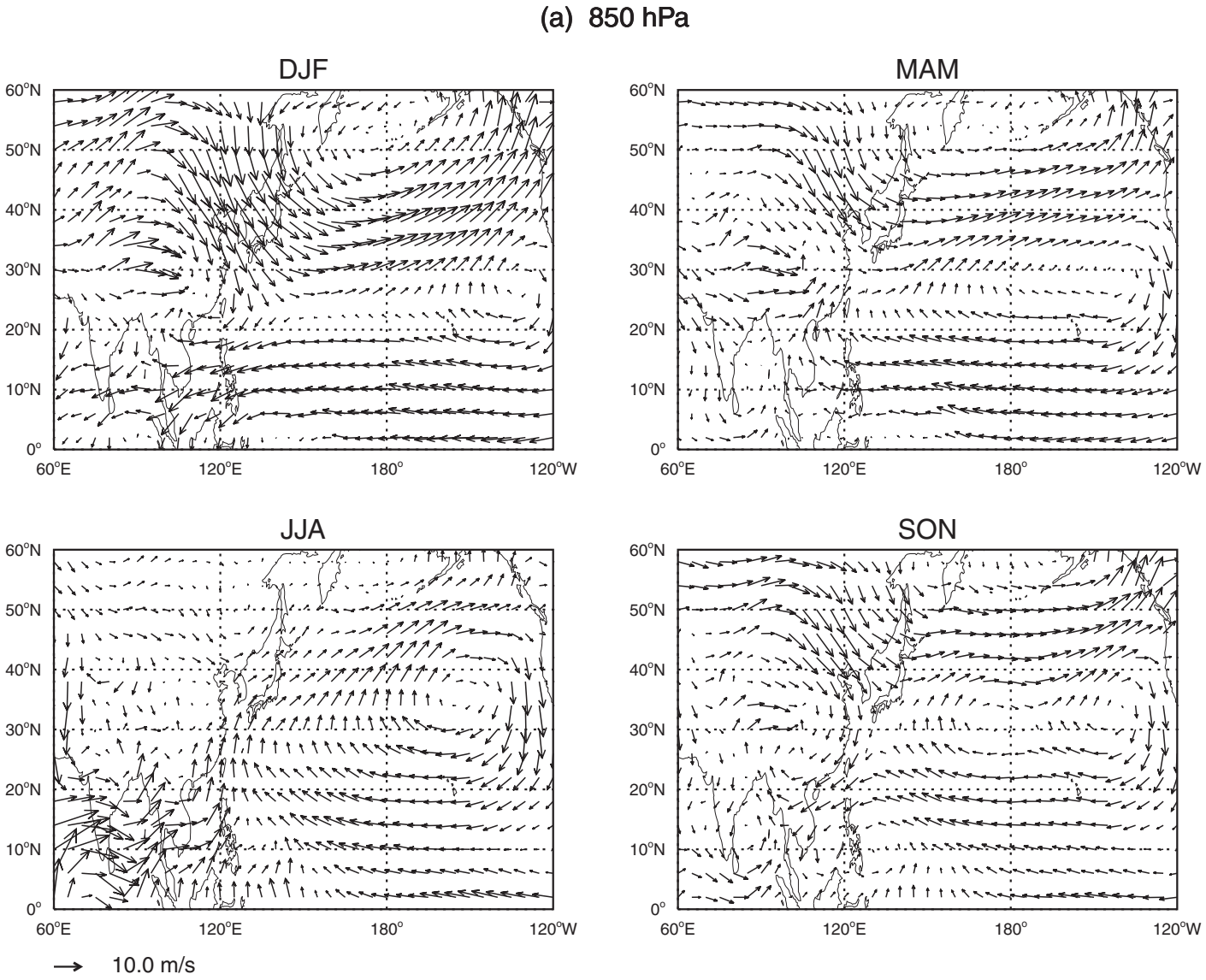

Figure 15: Mean wind fields by season derived from the GEOS-DAS data for the period 1991 - 2001 for a) 850 hPa.

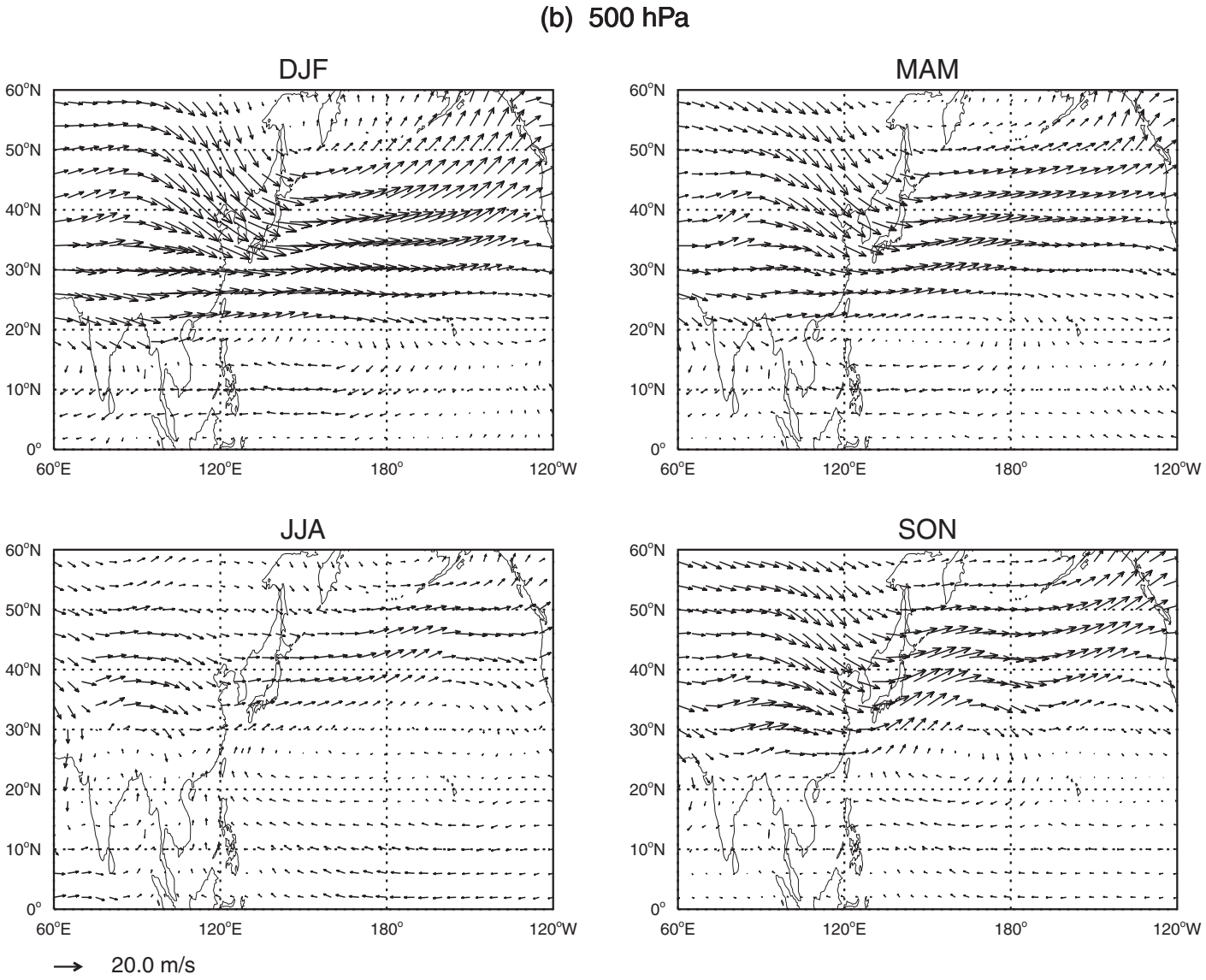

Figure 15: Mean wind fields by season derived from the GEOS-DAS data for the period 1991 - 2001 for b) 500 hPa.

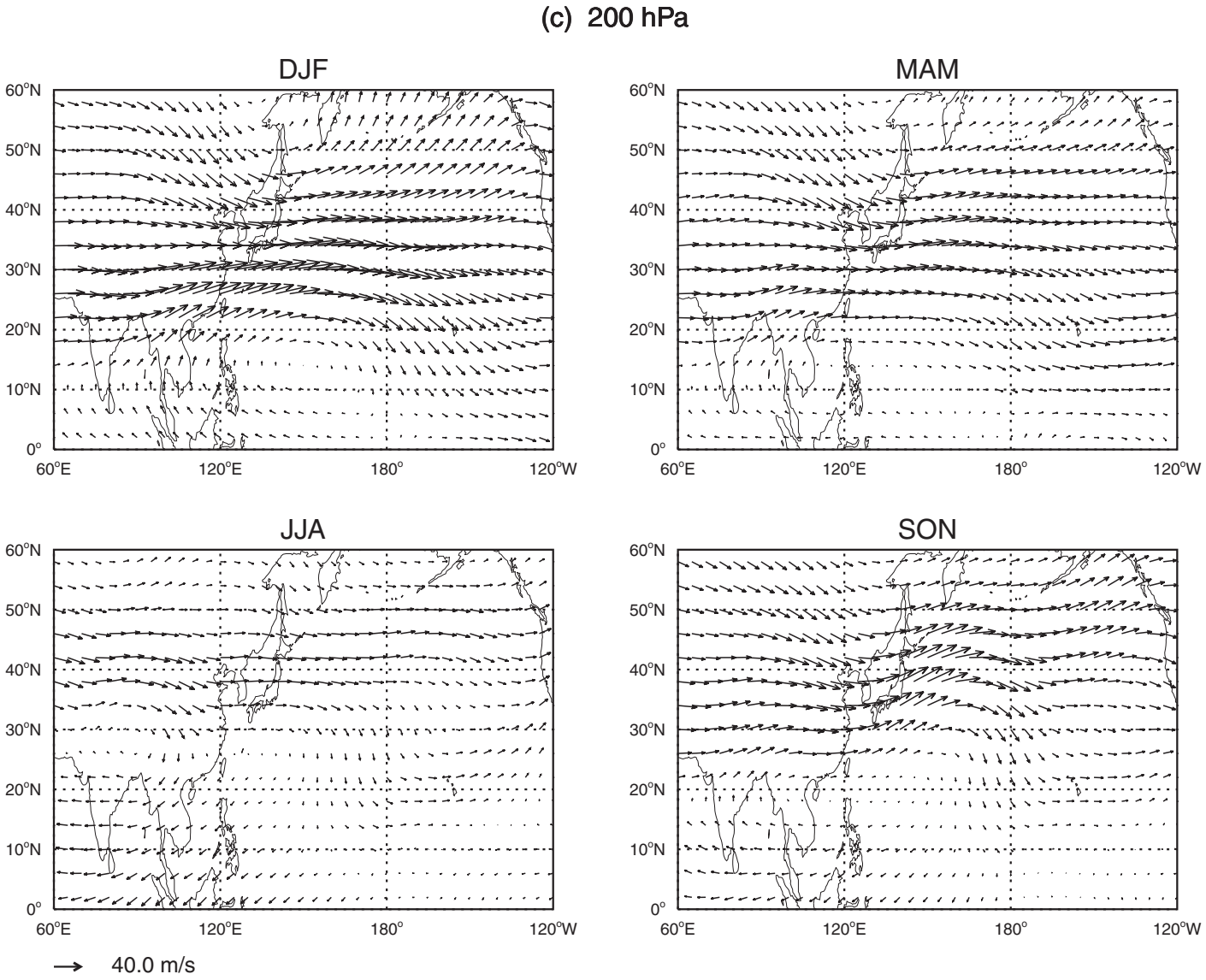

Figure 15: Mean wind fields by season derived from the GEOS-DAS data for the period 1991 - 2001 for c) 200 hPa.

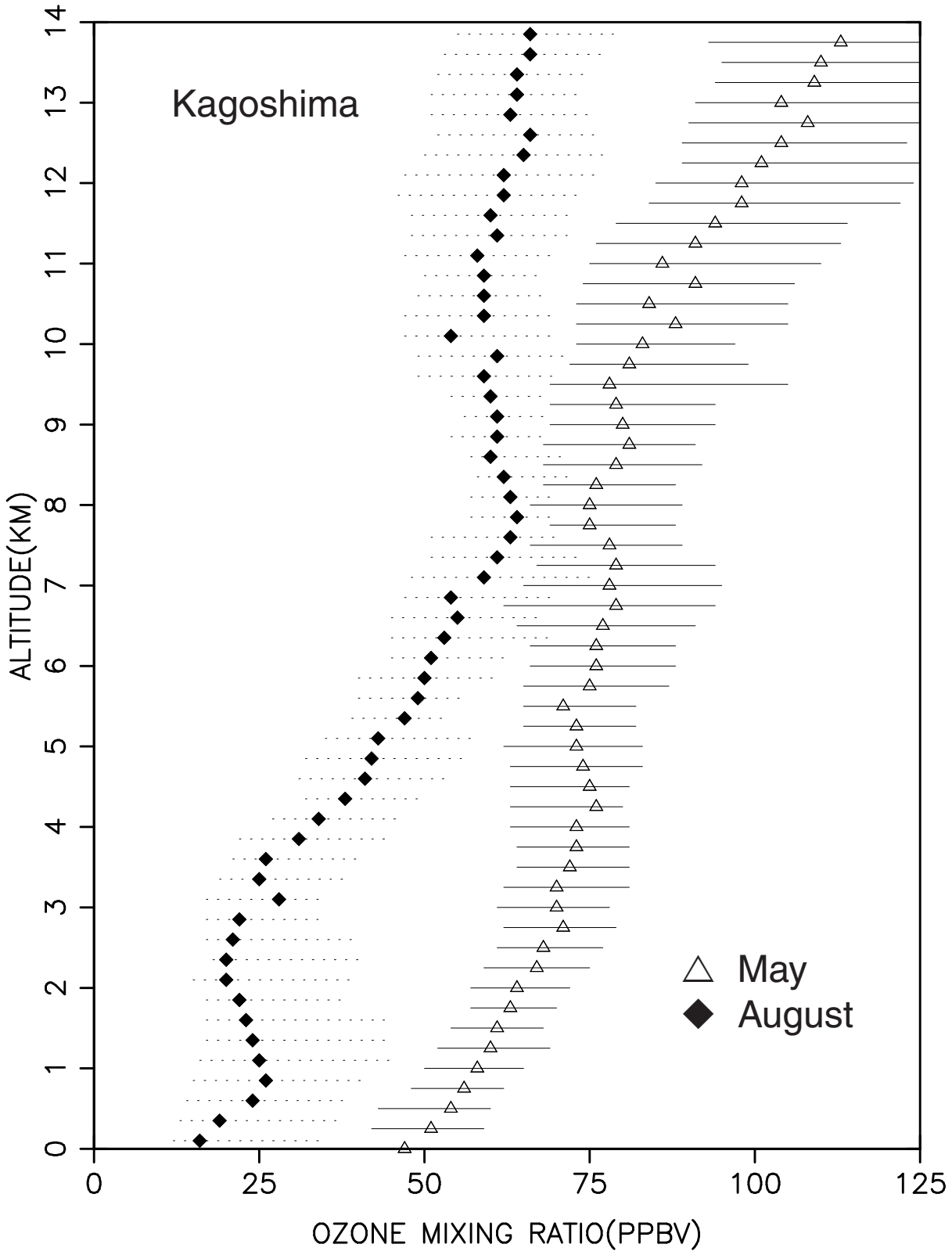

Figure 16: Median monthly tropospheric ozone mixing ratio for May (open triangle) and August (solid diamond) for Kagoshima, Japan. The solid and dotted horizontal lines are the inner 50th percentile of the mixing ratio at each 0.25 km altitude.

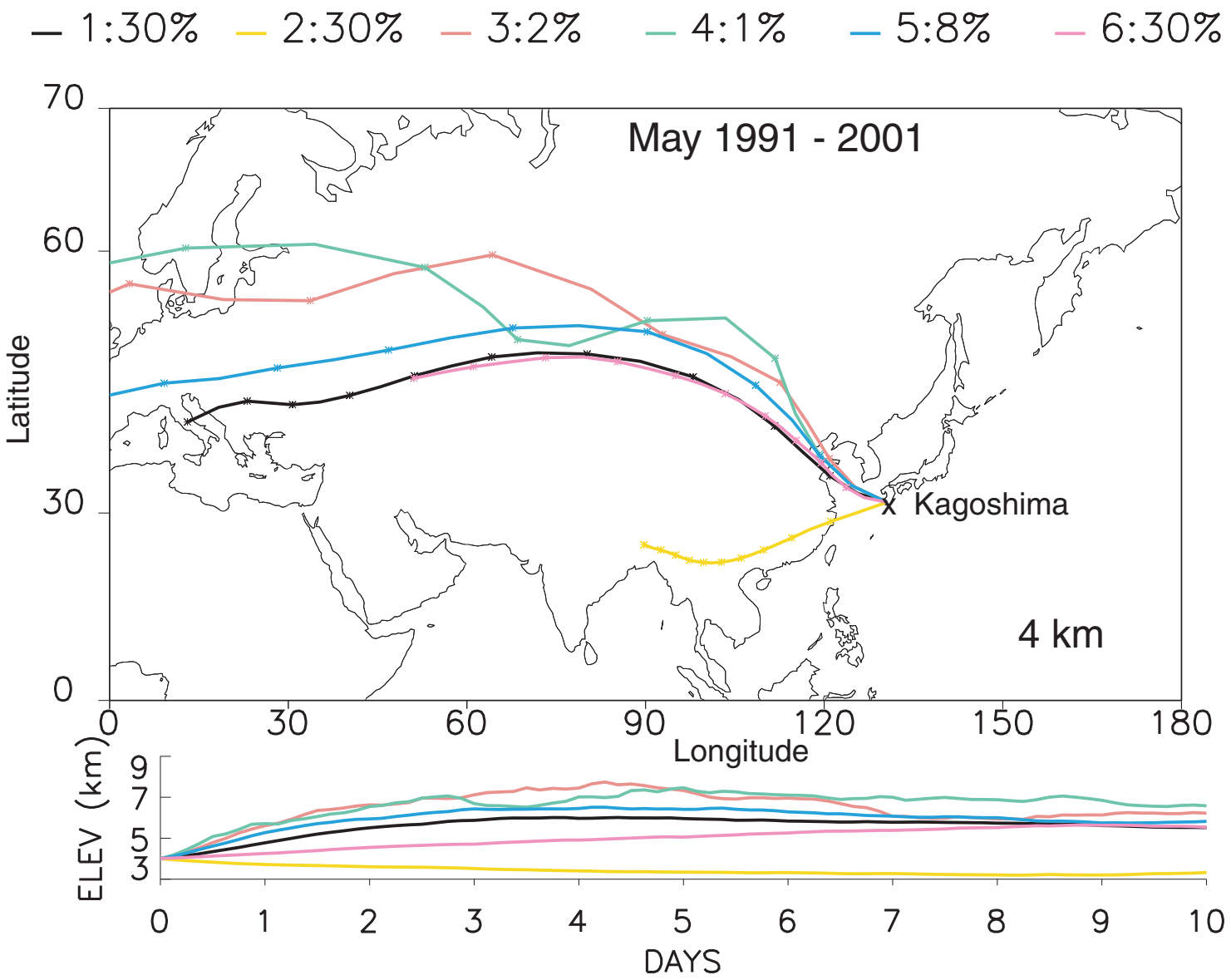

Figure 17a: Average air parcel trajectories at 4 km altitude at Kagoshima for May

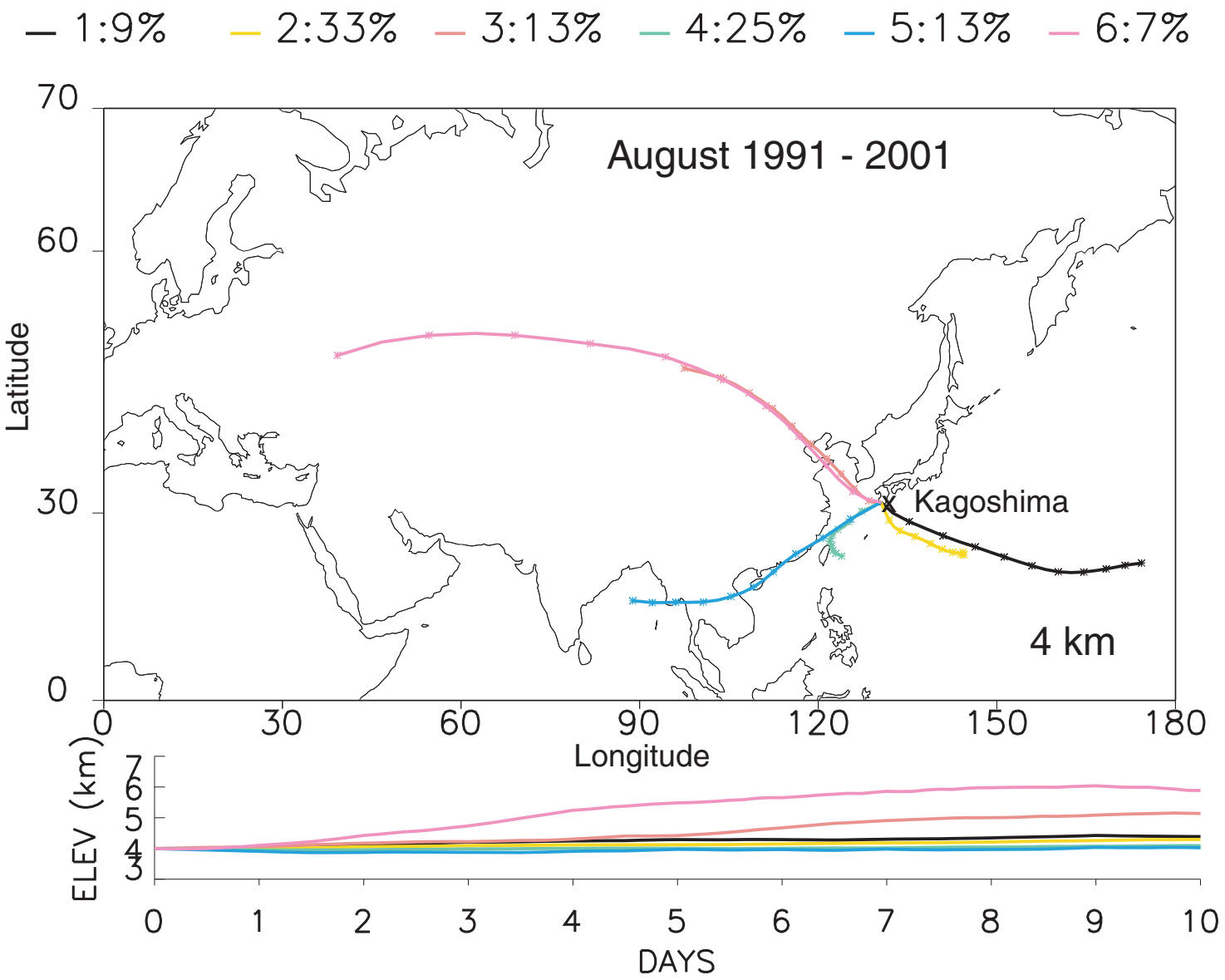

Figure 17b: Average air parcel trajectories at 4 km altitude at Kagoshima for August.

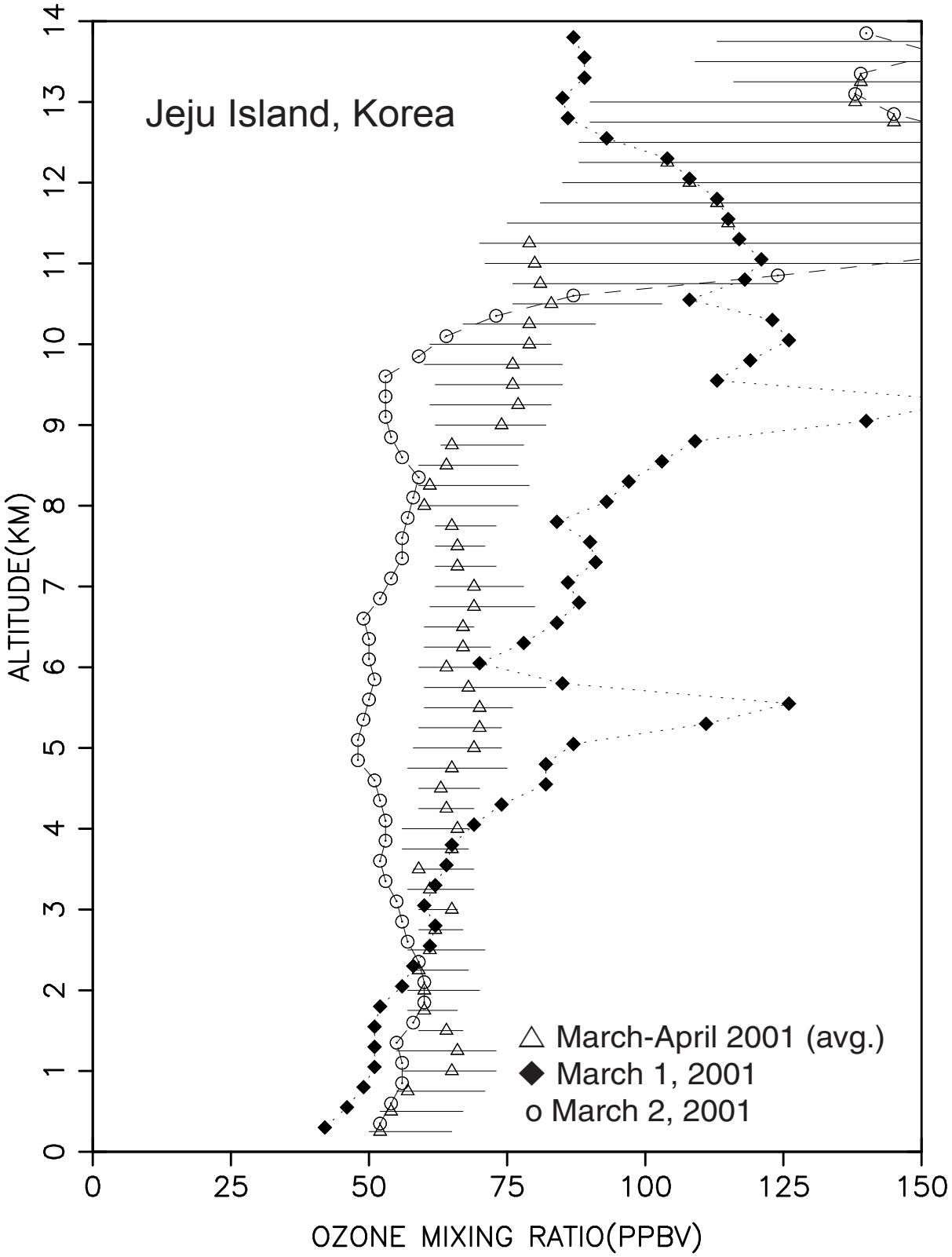

Figure 18: Profiles of ozone mixing ratio at Jeju Island on March 1, 2001 at 0415 GMT and March 2, 2001 at 0615 GMT with the March-April 2001 average.

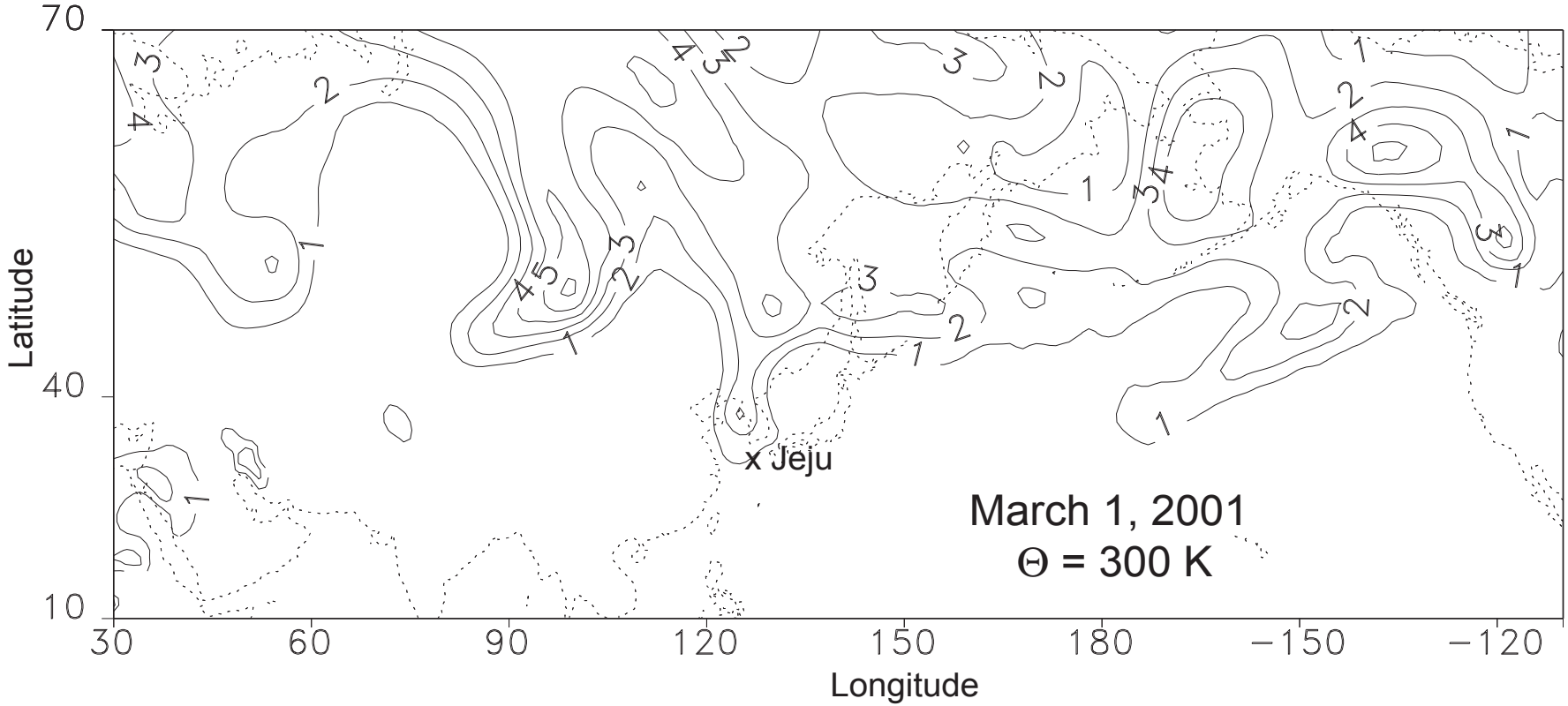

Figure 19a: Potential vorticity on March 1, 2001 at 0600 GMT on the 300 K potential temperature surfaces.

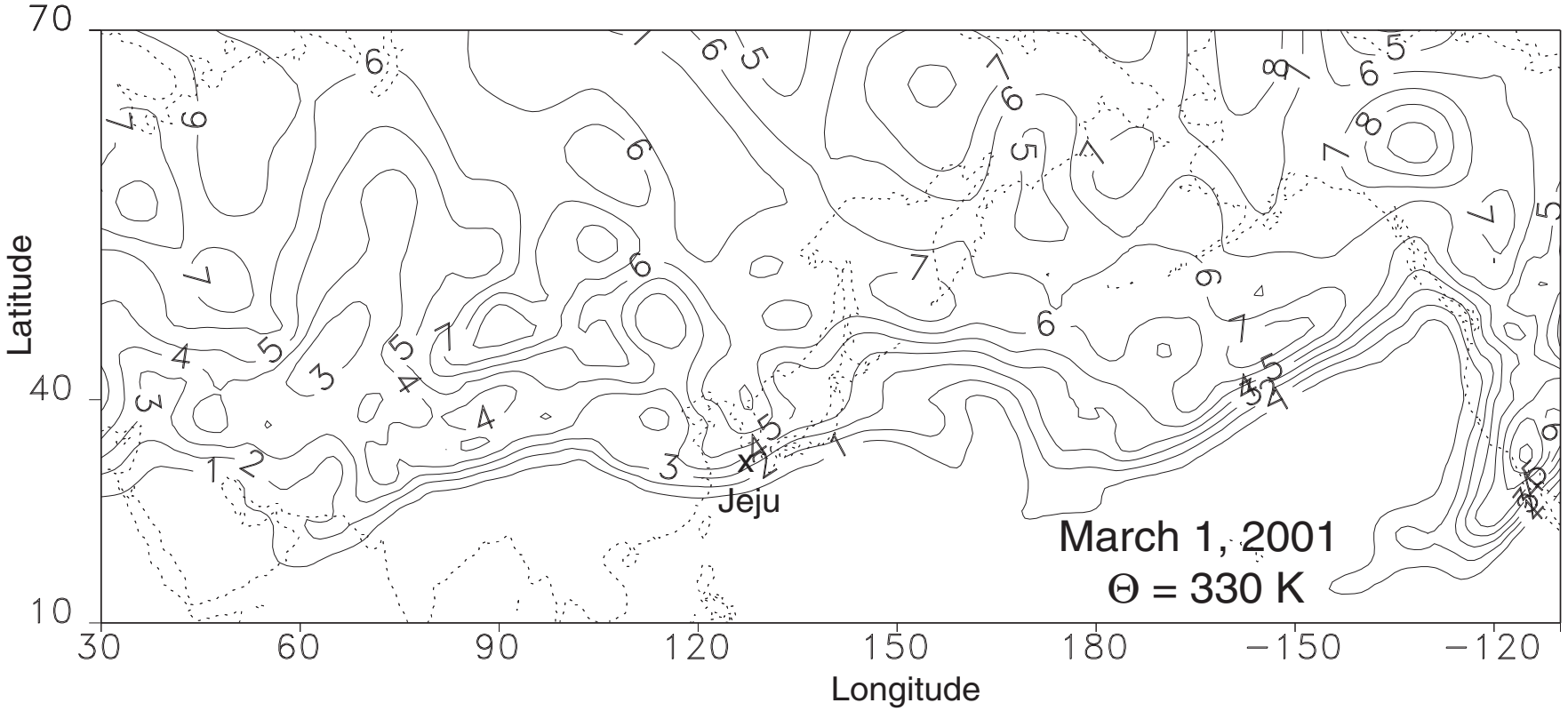

Figure 19b: Potential vorticity on March 1, 2001 at 0600 GMT on the 330 K potential temperature surfaces.

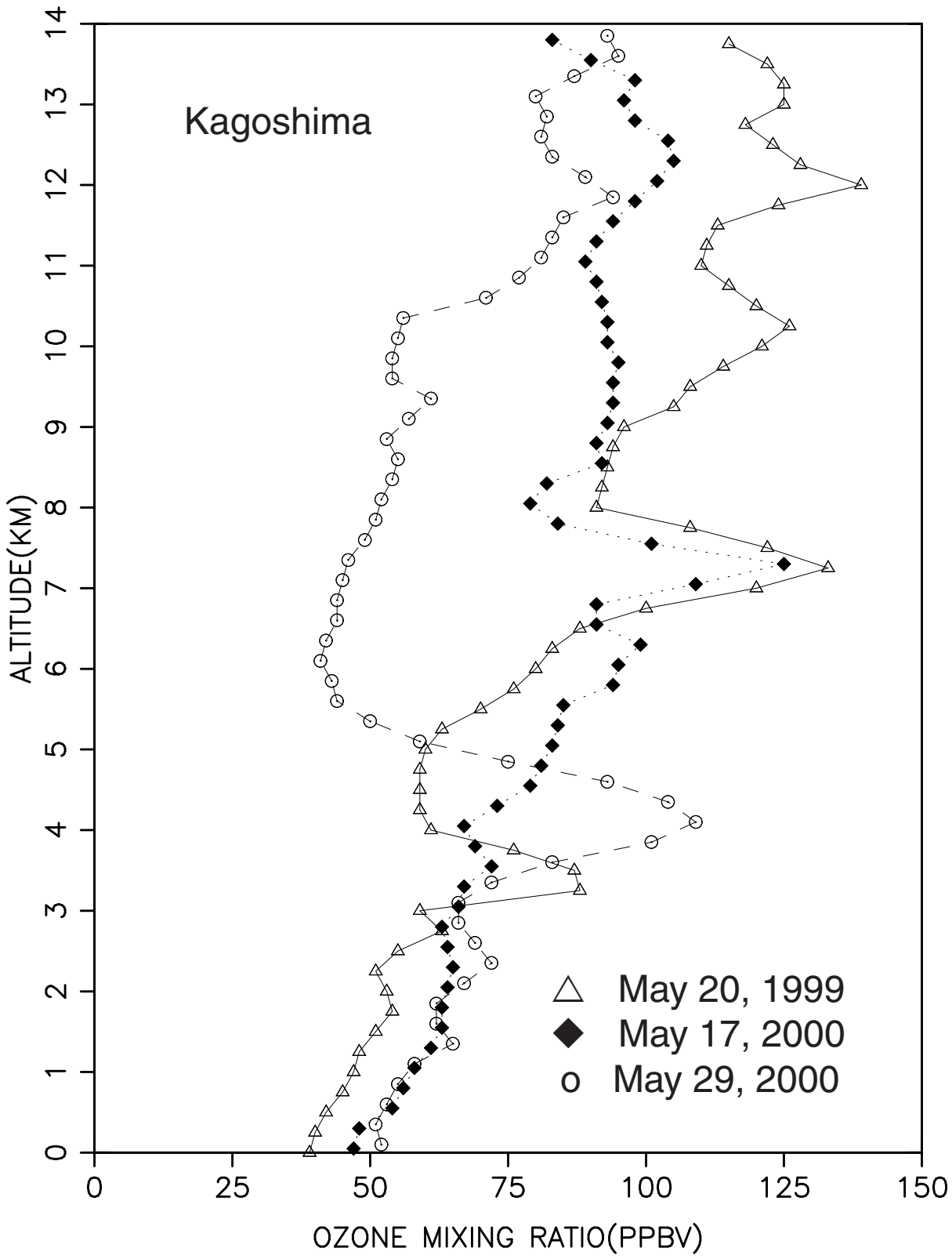

Figure 20: Profiles of ozone mixing ratio at Kagoshima on May 20, 1999, May 17, 2000, and May 29, 2000. The launch time of the ozonesonde for the three profiles was 1430 GMT.

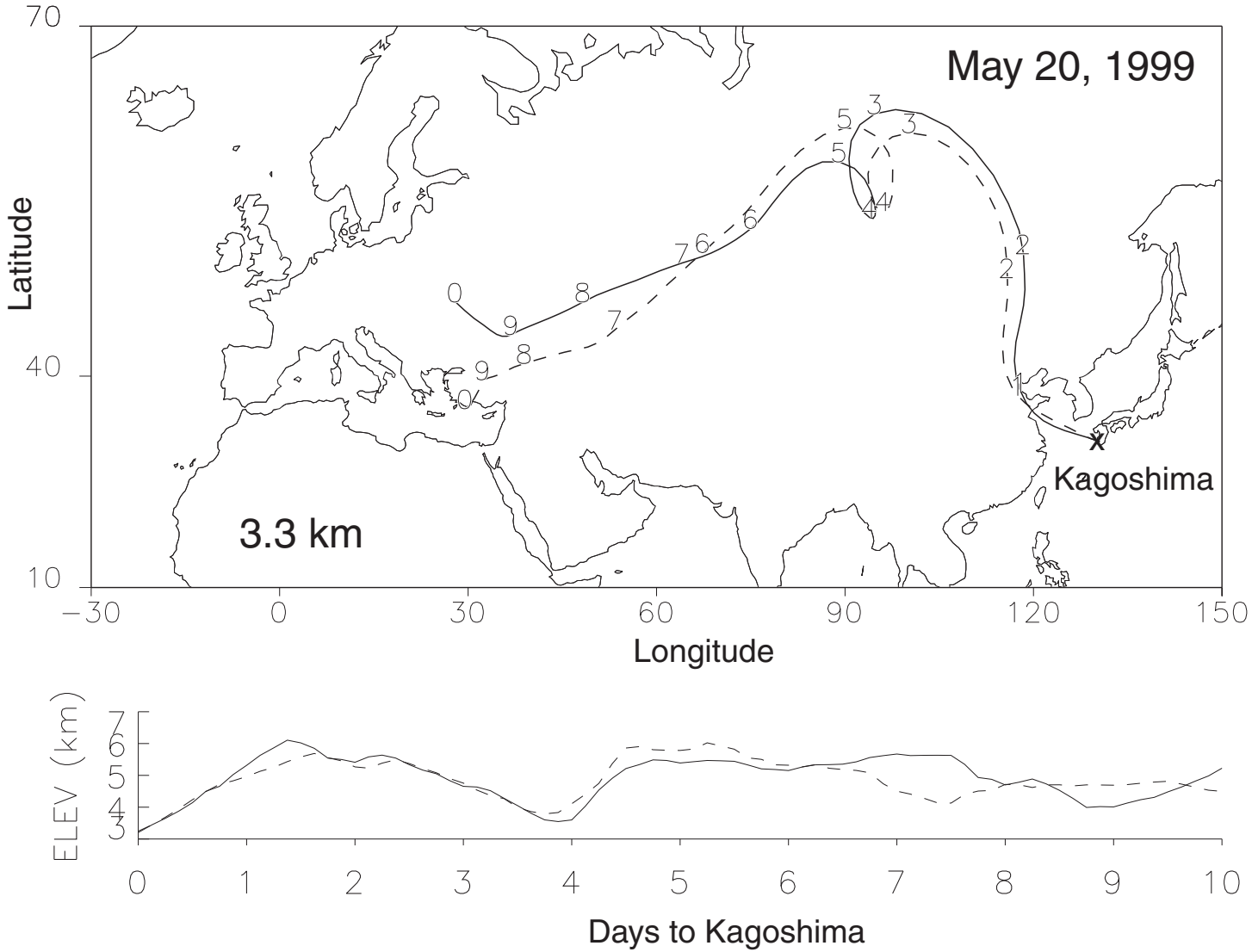

Figure 21: Isentropic 10-day back trajectory to Kagoshima on May 20, 1999 arriving at 3.3 km. The solid line is for the 1200 GMT trajectory and the dashed line for 1800 GMT.

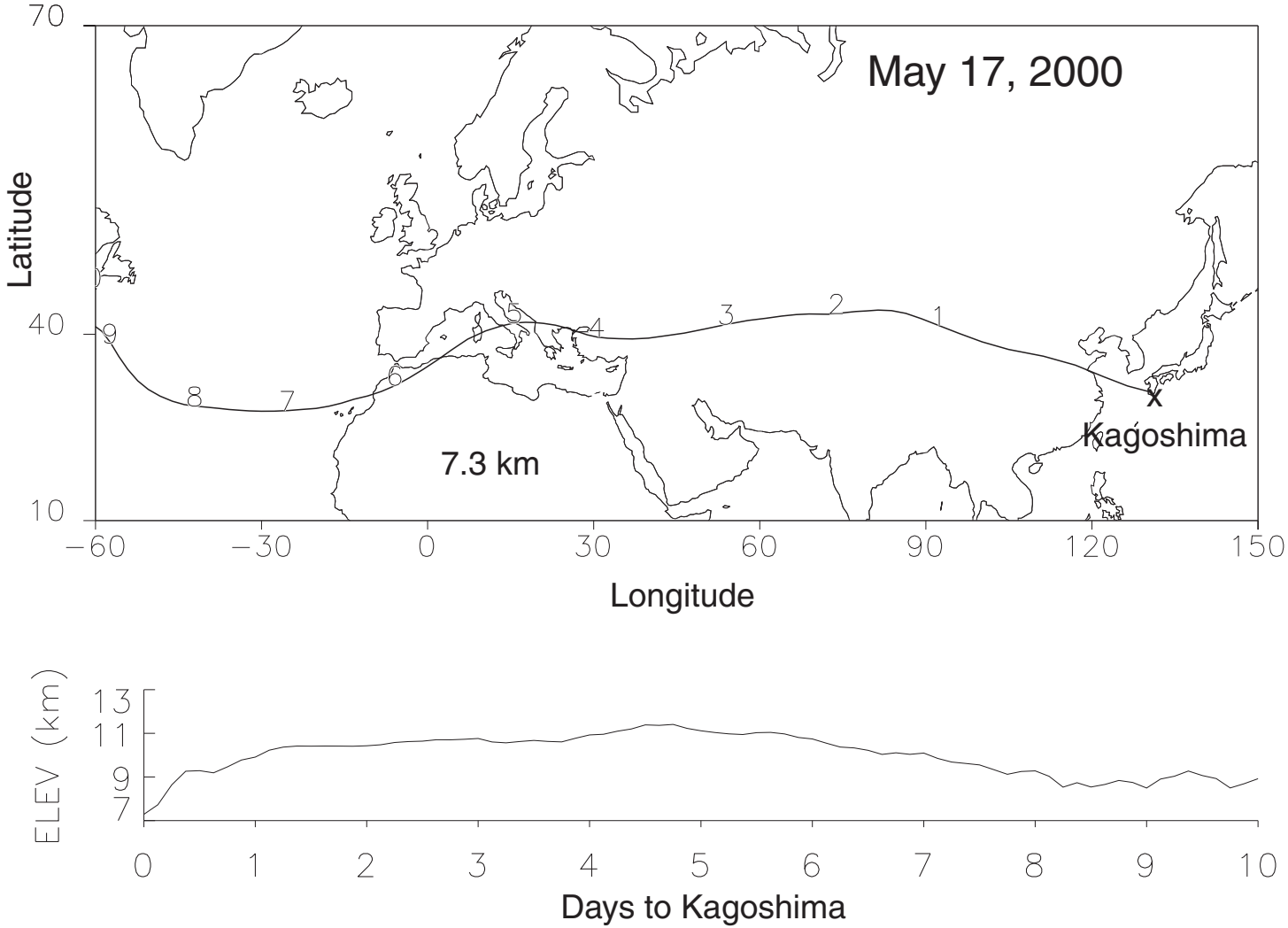

Figure 22: Isentropic 10-day back trajectory to Kagoshima on May 17, 2000 arriving at 7.3 km at 1800 GMT.

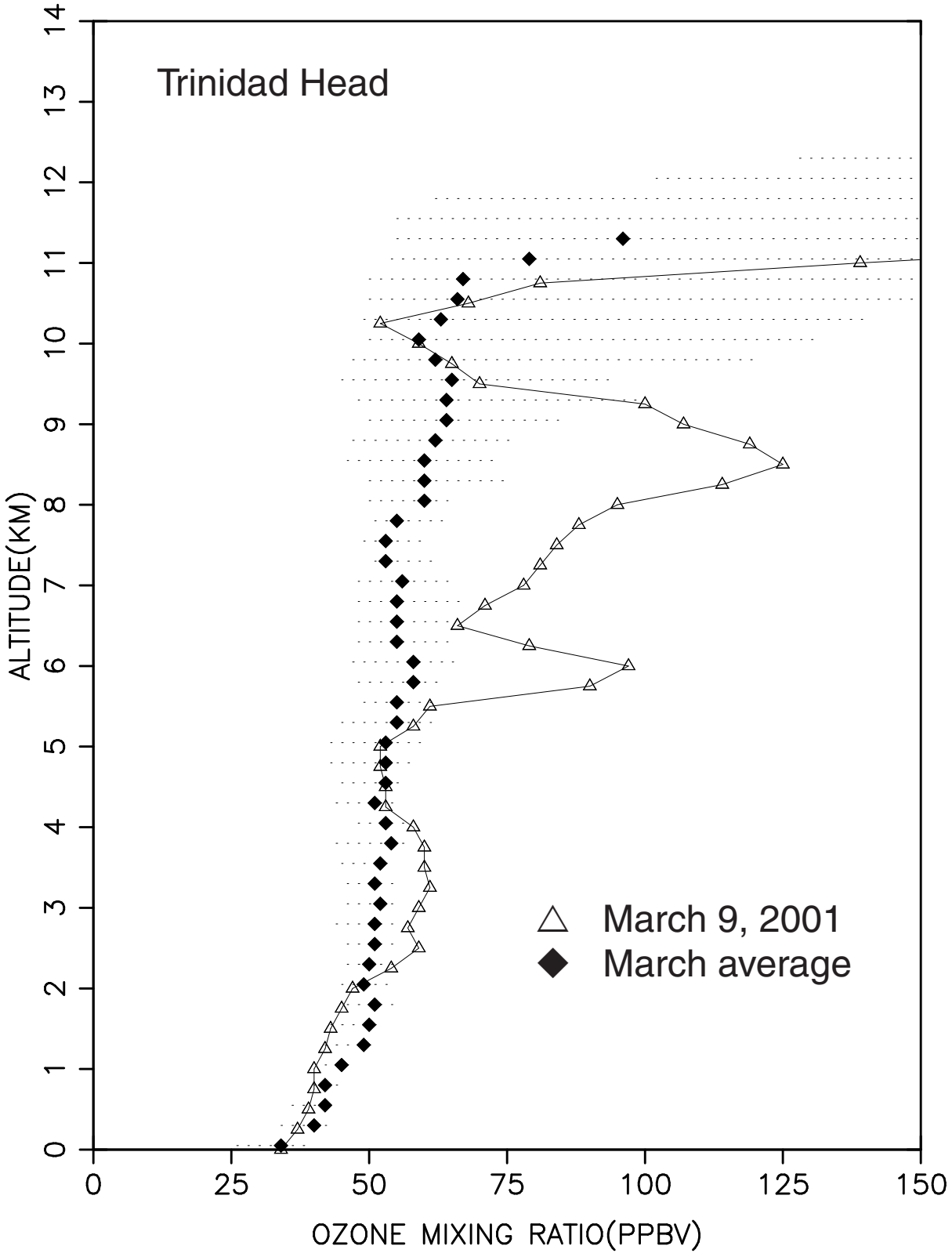

Figure 23: Profile of ozone mixing ratio at Trinidad Head on March 9, 2001 at 1800 GMT. The multiyear median profile for March is also shown.

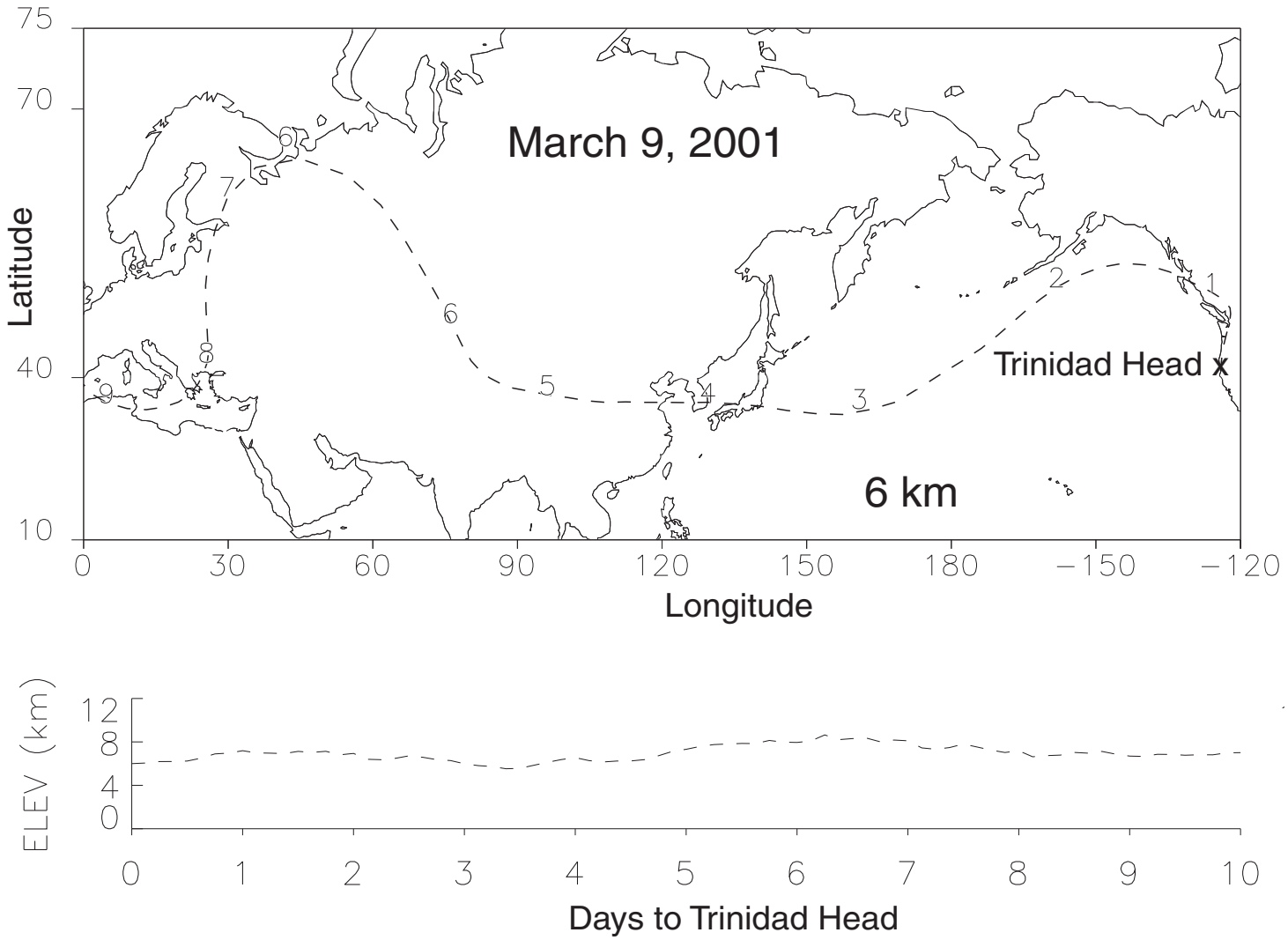

Figure 24: Isentropic 10-day back trajectory to Trinidad Head on March 9, 2001 at 1800 GMT arriving at 6 km.

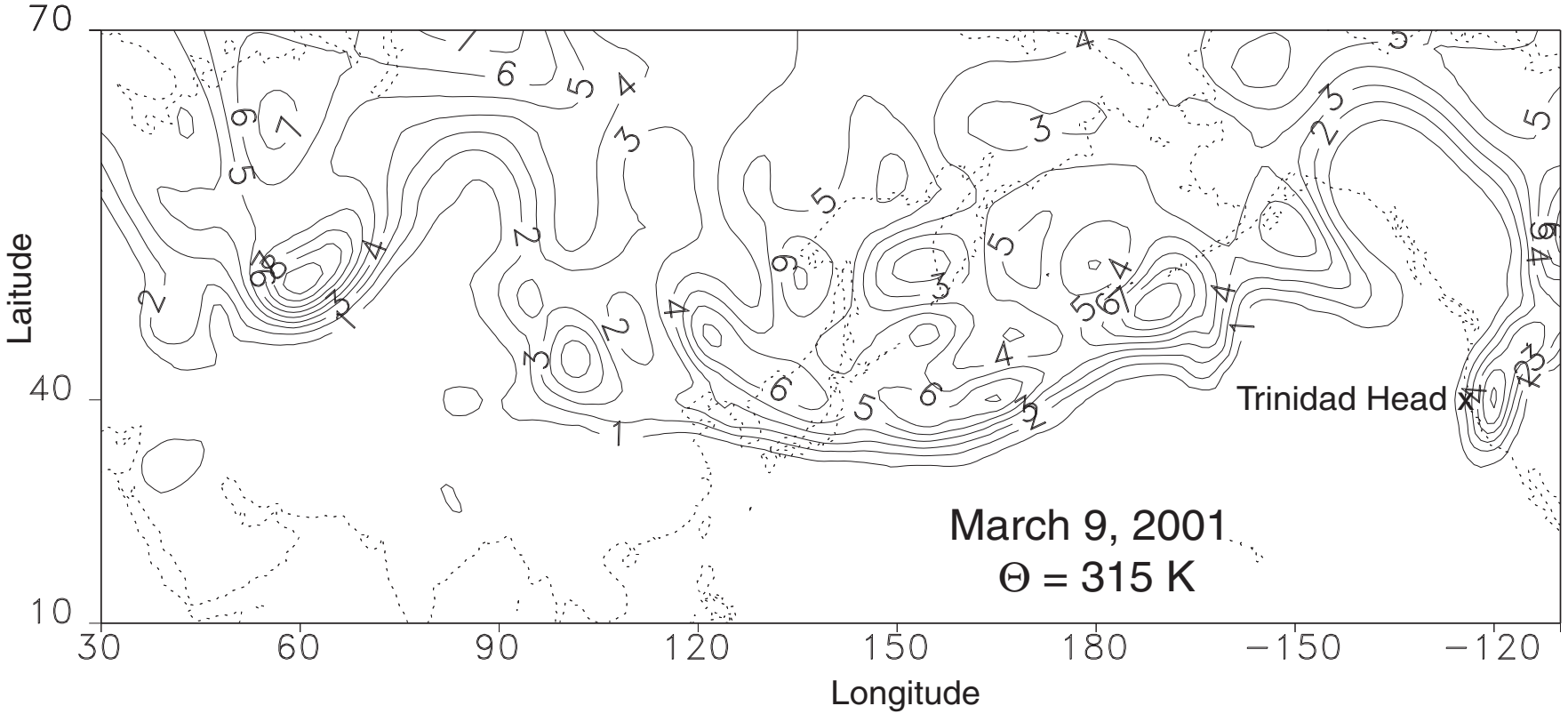

Figure 25: Potential vorticity on March 9, 2001 at 1800 GMT on the 315 K potential temperature surface.

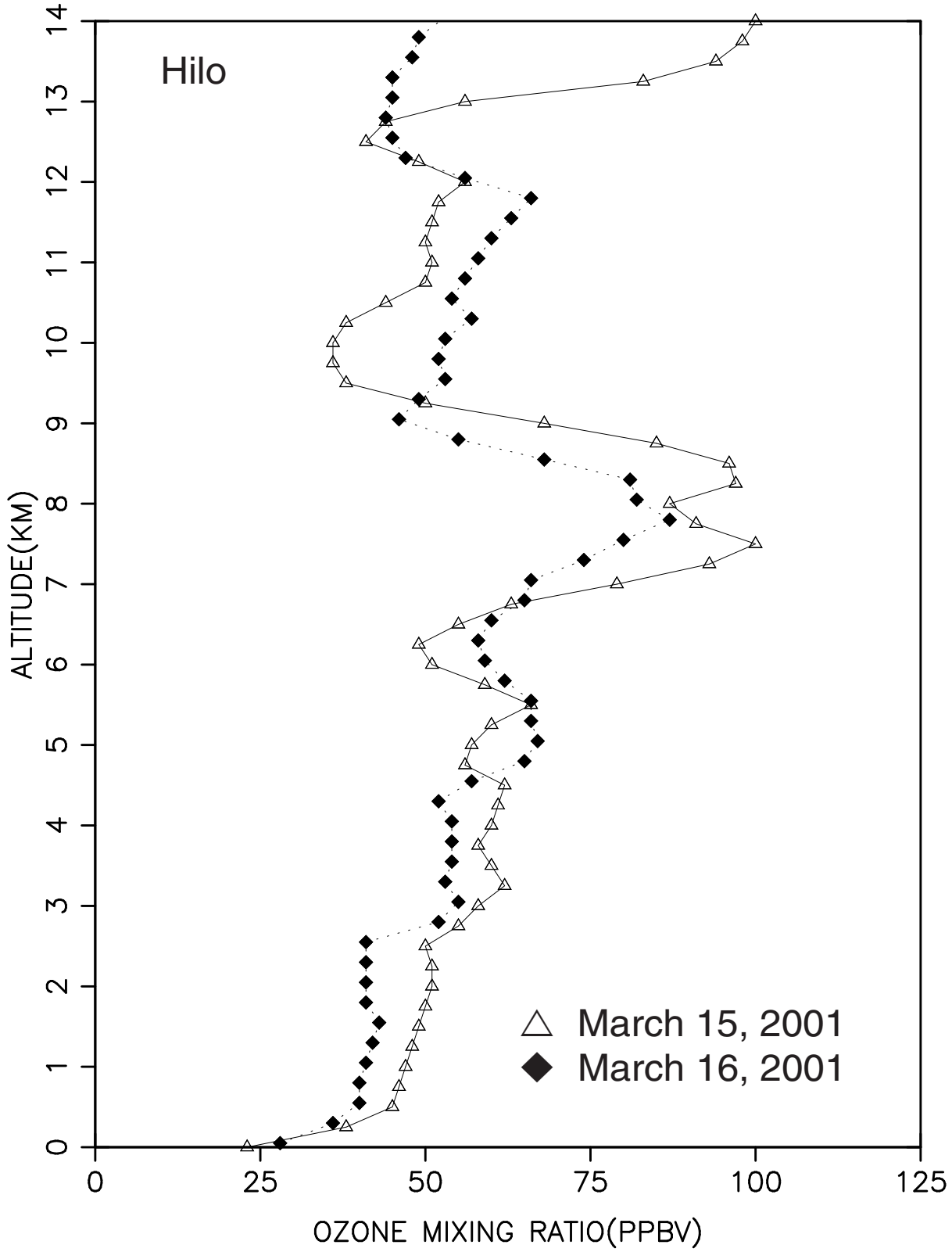

Figure 26: Profiles of ozone mixing ratio at Hilo March 15 and 16, 2001. The launch time of the ozonesonde for the two profiles was 1830 GMT.

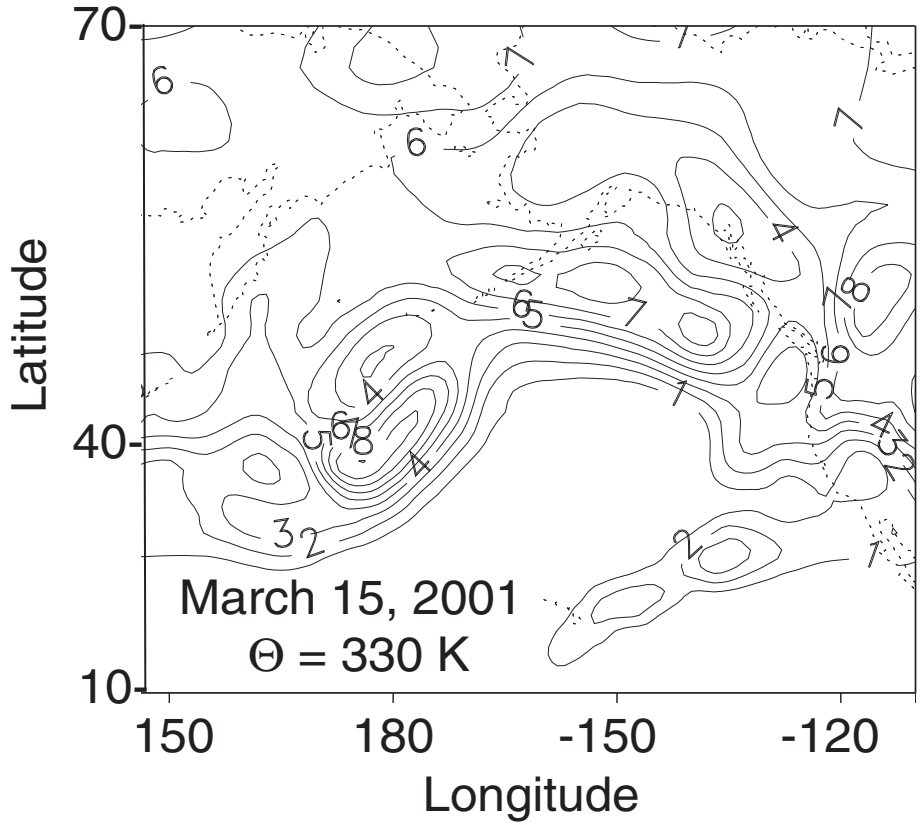

Figure 27: Potential vorticity on March 15, 2001 at 1800 GMT on the 330 K potential temperature surface.

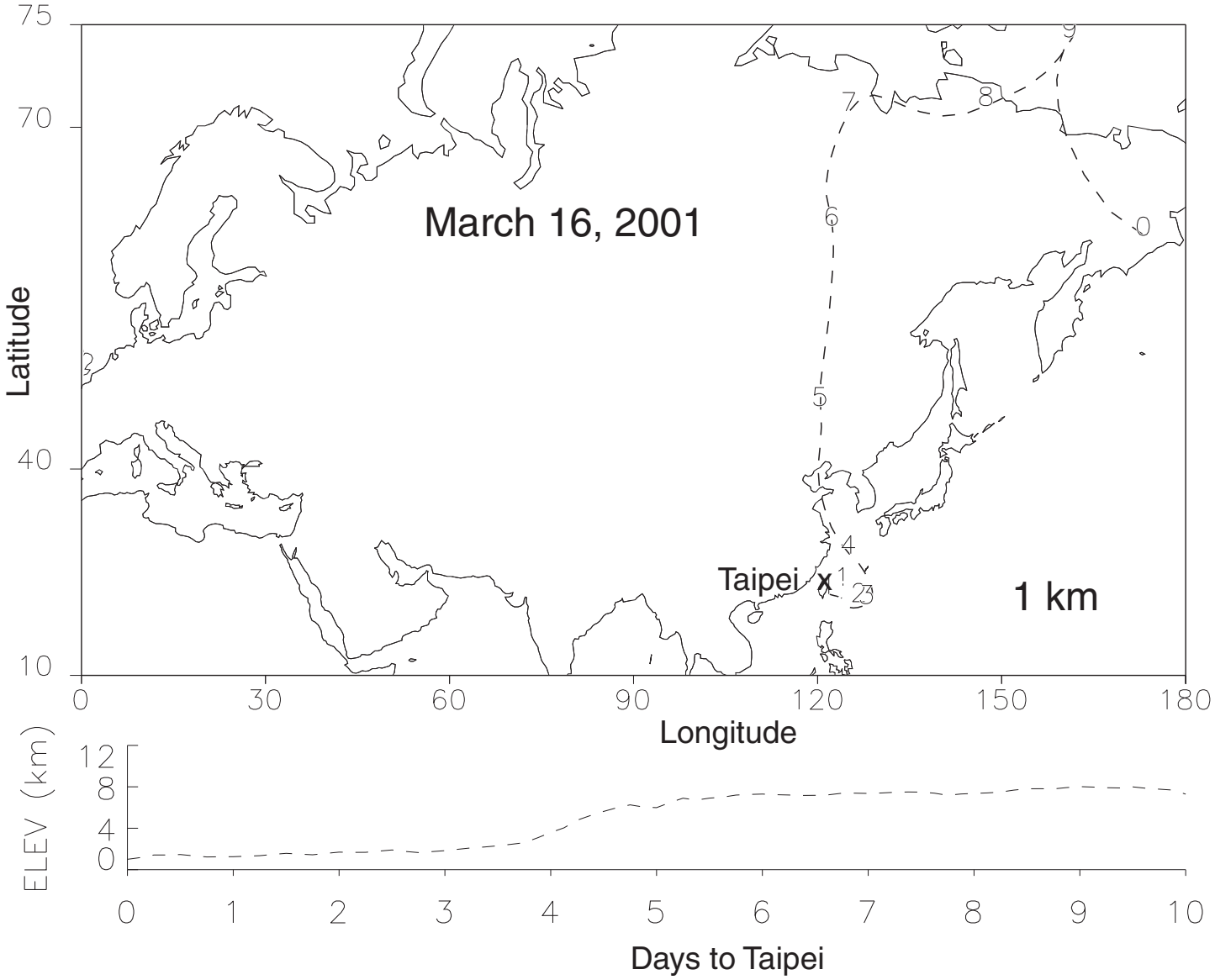

Figiure 28: Isentropic 10-day back trajectory to Taipei on March 16, 2001 at 0060 GMT at 1 km.

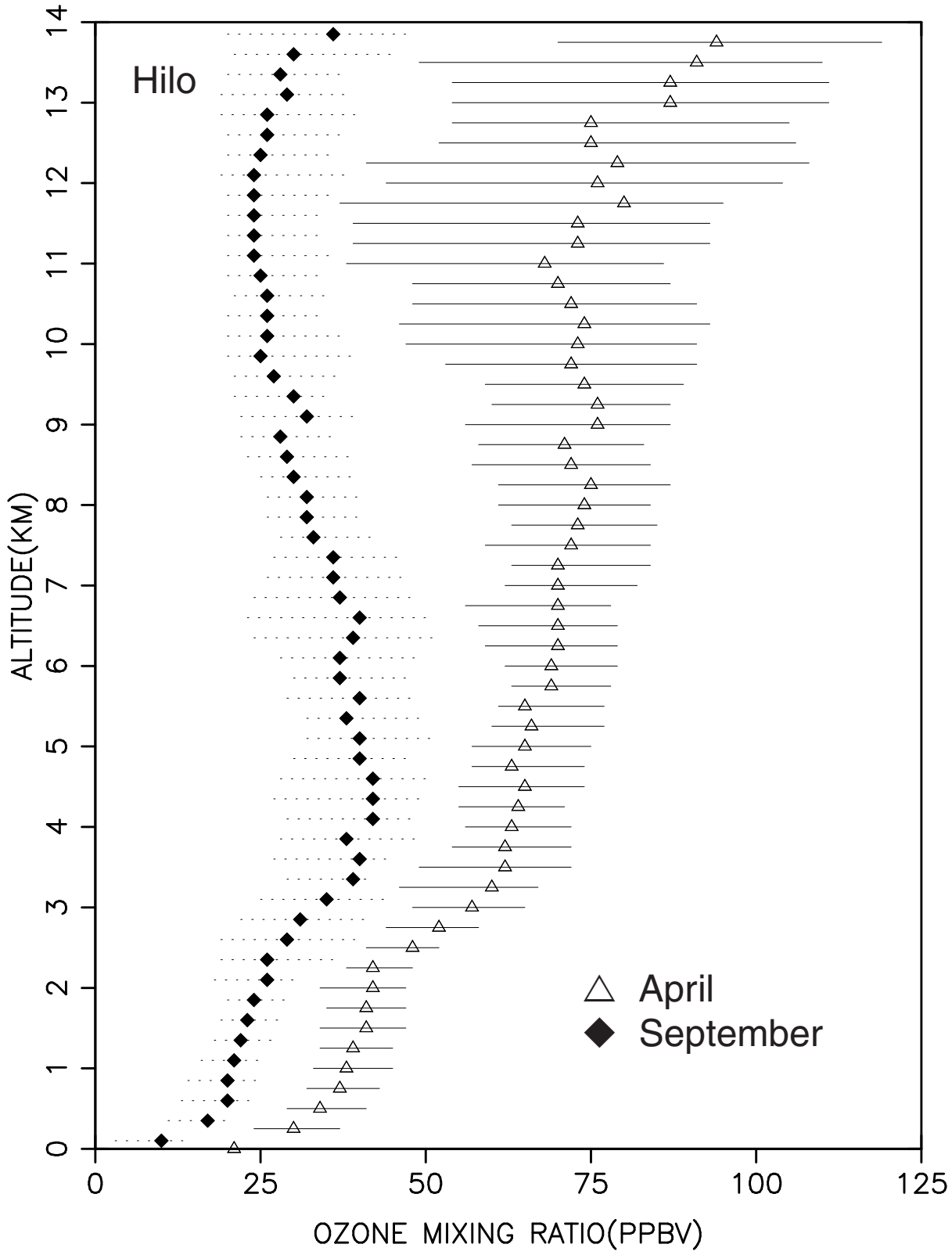

Figure 29: Median monthly tropospheric ozone mixing ratio for April (open triangle) and September (solid diamond) for Hilo, Hawaii.

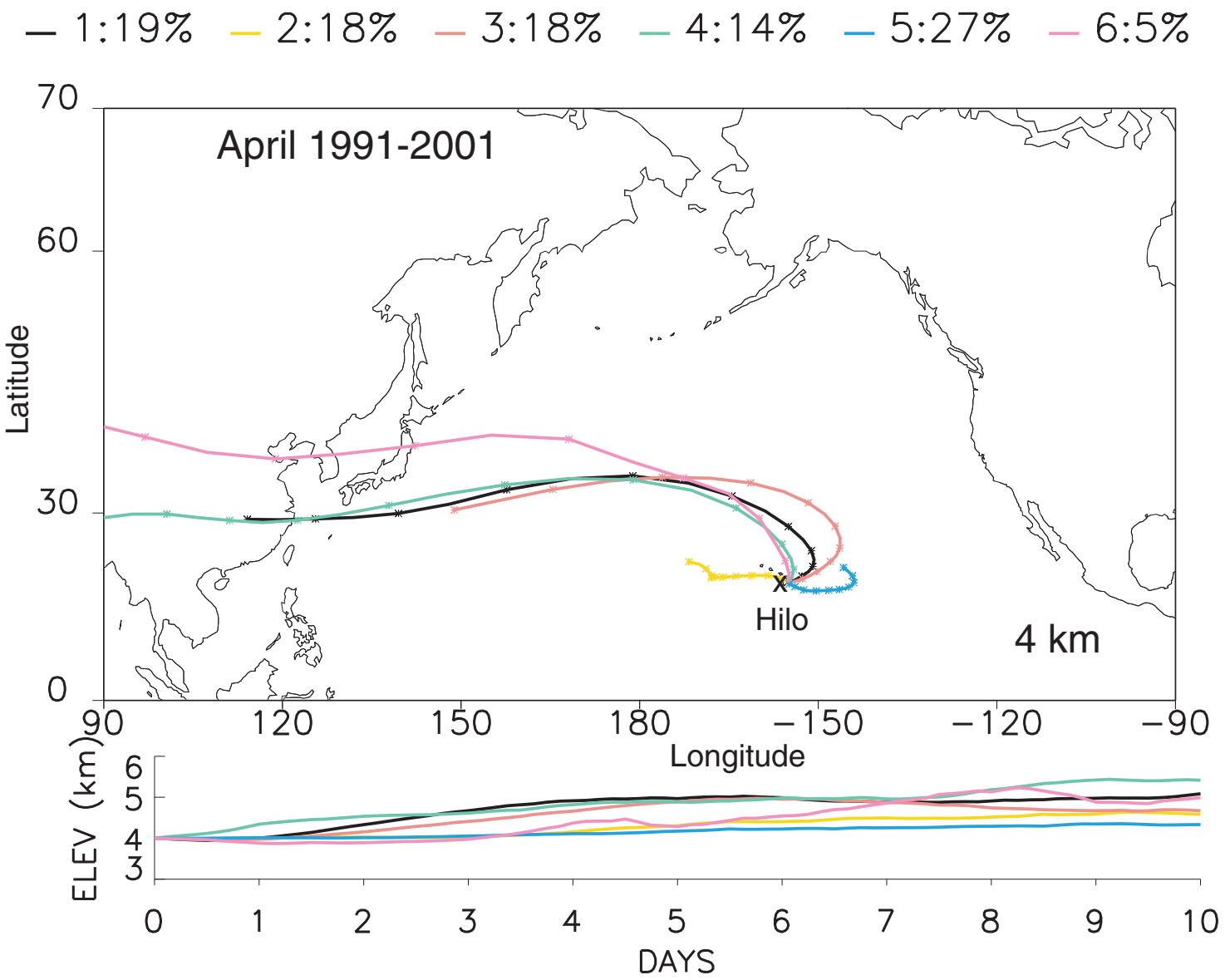

Figure 30a: Average air parcel trajectories at 4 km altitude at Hilo for April.

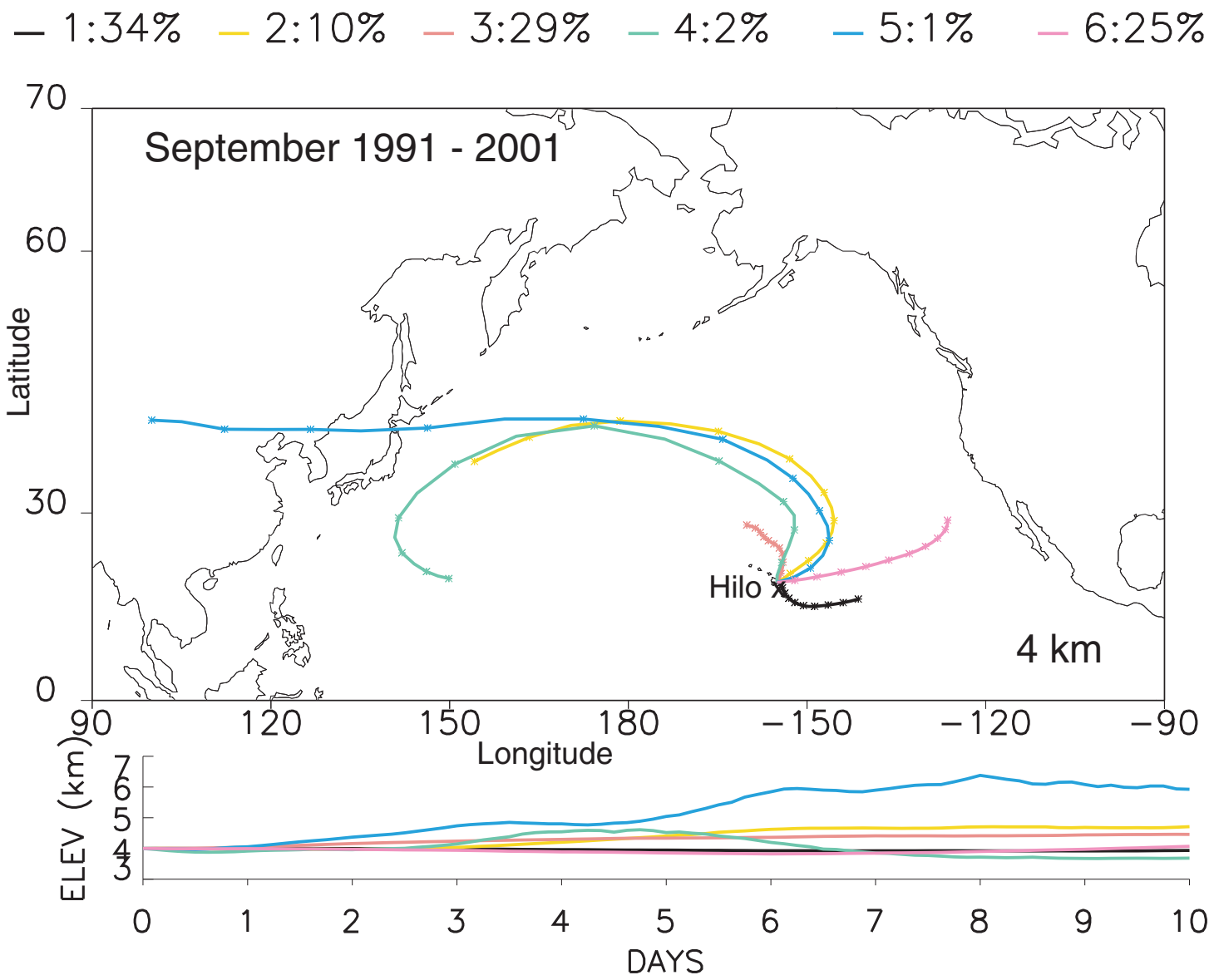

Figure 30b: Average air parcel trajectories at 4 km altitude at Hilo for September

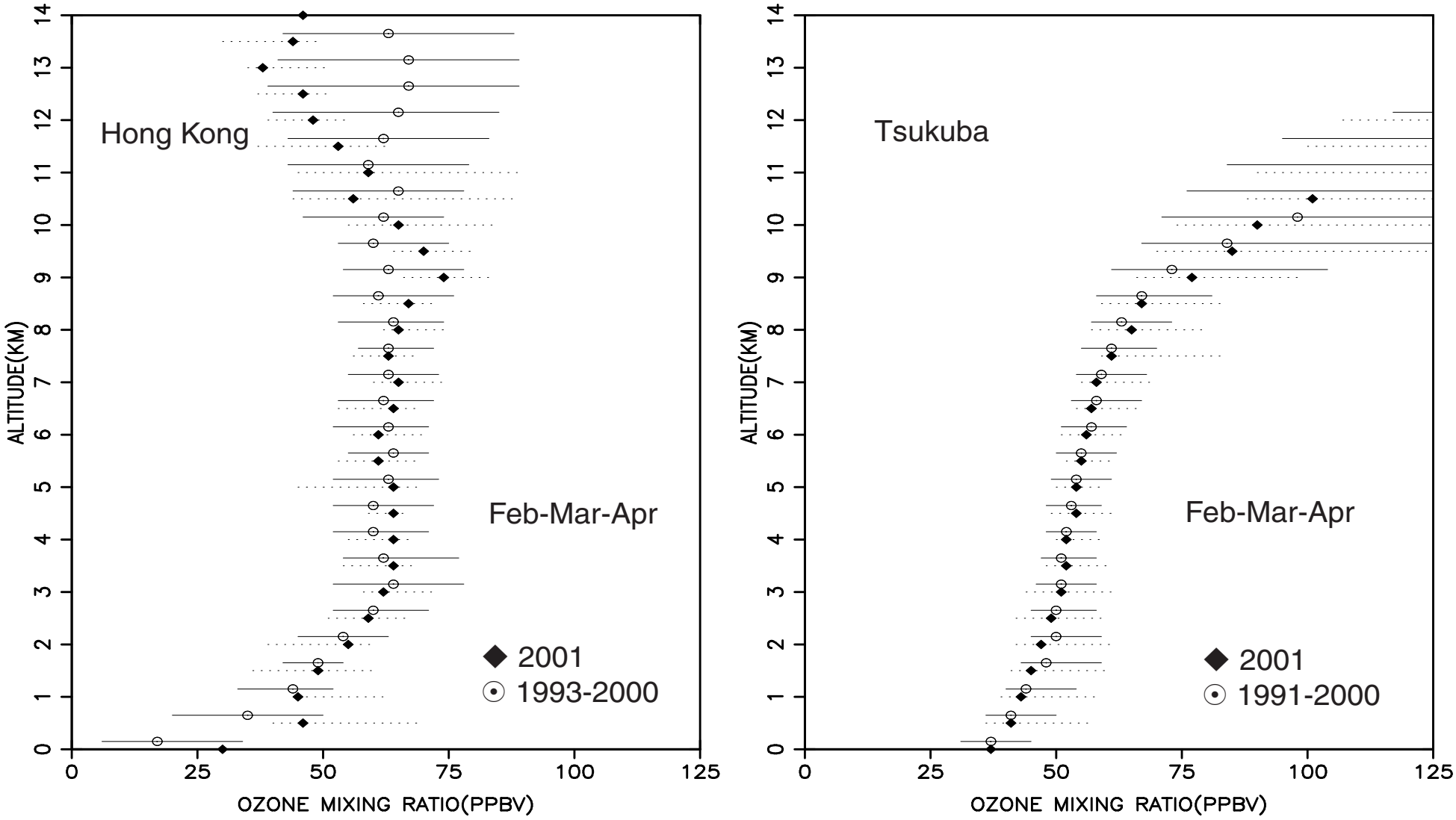

Figure 31: Comparison of the February-March-April 2001 median ozone mixing ratio profiles with the long-term average for Hong Kong and Kagoshima.